# Final Report

for

# Novel Membrane and Electrodeposition-Based Separation and Recovery of Rare Earth Elements from Coal Combustion Residues

DE-FE0026952

Project Period:
March 1, 2016 to February 28, 2018

REPORT PREPARED BY:

Heileen Hsu-Kim, Duke University
Desiree Plata, Yale University
James C. Hower, University of Kentucky
Zachary Hendren, RTI International
Mark Wiesner, Duke University

SUBMITTED BY
Duke University
121 Hudson Hall, Box 90287
Durham, NC 27708

PRINCIPAL INVESTIGATOR
Heileen Hsu-Kim, Ph.D.
Phone: +1(919) 660-5200
hsukim@duke.edu

SUBMITTED TO
U.S. Department of Energy
National Energy Technology Laboratory

Acknowledgment: "This material is based upon work supported by the Department of Energy under Award Number DE-FE0026952."

**Table of Contents**

## 1. Executive Summary

This project developed a hydrometallurgical-based technology to extract and concentrate rare earth elements (REEs) from a representative group of coal combustion residuals (CCRs) from major coal sources in the United States. The approach for REE recovery comprises two general components: (1) Leaching of REEs from CCRs and (2) Separation of REEs from other major ions in the CCR leachate. The leaching step entails acid leaching with nitric or hydrochloric acid, and in some cases, pretreatment of CCRs with alkaline roasting prior to acid leaching. The follow-up REE recovery steps involve a series of membrane-based methods to separate and concentrate rare earth ions from other major ions in acid leachates of CCRs. These methods include liquid emulsion membranes, supported liquid membranes and electrodeposition with carbon nanotube electrochemical filters. The advantage of these separation approaches (relative to conventional approaches such as solvent extraction) is a reduction in the usage of solvents and other costly chemicals and a reduction of hazardous waste products that are challenges in conventional REE separation methods. In the testing of our process, we selected a representative set of CCR samples from our collection and performed a suite of characterization measurements (total REE content and major mineralogy). The major results of this work demonstrated that heated acid leaching could efficiently extract REEs from PRB-based coal fly ashes while the Appalachian and Illinois Basin CCRs required alkaline roasting with NaOH prior to acid leaching at room temperature. The supported liquid membrane (SLM) configuration and electrochemical deposition (ED) system yielded the most promising methods of REE recovery from the acid leachates of fly ash. Our most concentrated product to date comprised 1 wt.% (dry basis) REEs produced from an Appalachian-based fly ash leached and purified by SLM. The SLM separation process was more selective for heavy REEs over the light REEs. When SLM was combined with ED, preliminary results demonstrated that a final product of >2 wt.% REEs was possible.

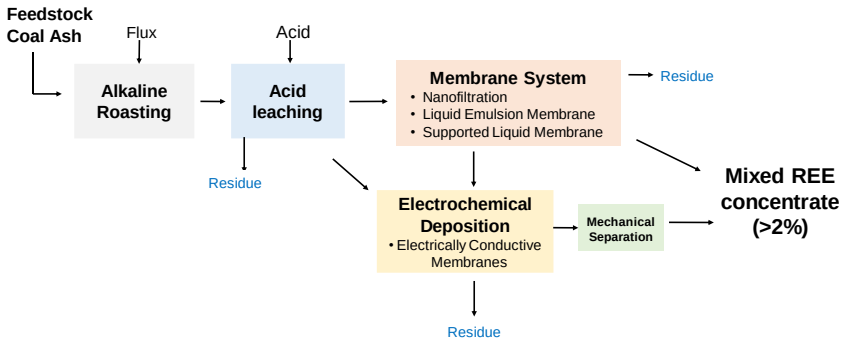


**Figure 1.1.** This project investigated membrane-based hydrometallurgical technologies to separate and concentrate REEs from coal combustion residuals. The novelty of our approach is the application of liquid membranes and electrochemical deposition for the separation of REEs from acid leachates.

## 2. Feedstock Characterization

### 2.1 Rationale for Selection

Coal combustion residues (also referred as *coal ash*) include fly ash, bottom ash, and sludge from flue gas desulfurization scrubbers and are typically enriched in metals such as REEs. The selection of feedstock for our REE recovery technology is based on previous work (Taggart

et al. 2016) documenting the REE contents of more than 100 coal combustion fly ash samples as well as 20 samples of other types of CCRs (bottom ash, mechanical fly ash, silo ash, and ash from landfills and disposal ponds). The samples were collected in the timeframe between 1994 and 2015 from 22 U.S. coal-fired power plants that were burning a variety of coals from the major coal-producing regions in the United States (Appalachian, Illinois, Powder River, San Juan, and Gulf Coast Basins). Non-parametric statistical tests were used to discern trends in REE contents as a function of coal ash characteristics including the coal basin and major oxide content. For example, fly ashes with greater Al-oxide content (such as Appalachian-based coal ashes) generally have greater amounts total REEs (Figure 2.1) (Taggart et al. 2016). We also observed that a greater proportion of the REEs in Powder River Basin fly ashes was leached into nitric acid, and this may be due to the material containing more acid-reactive mineral phases (i.e. Ca-oxides) that can facilitate the liberation of REEs from the ash particles.

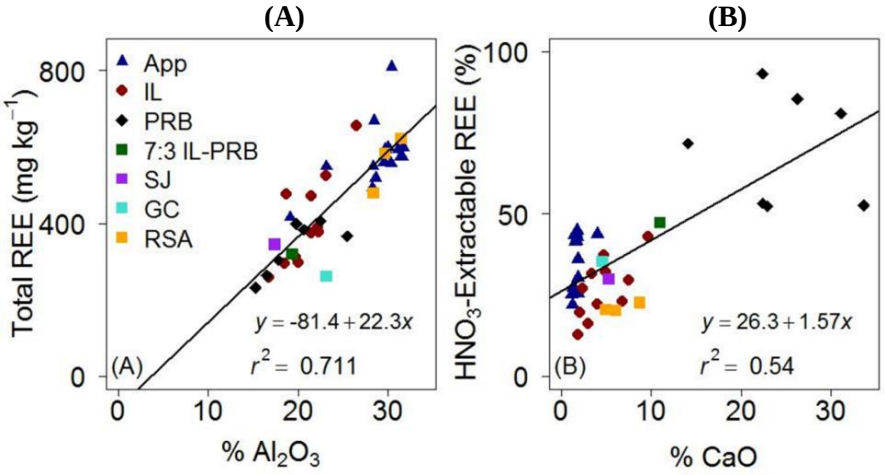


**Figure 2.1.** Total and extractable REE content of coal fly ashes depend on the fractions of major elements comprising the ash. (A) Higher aluminum content (as observed in Appalachian basin fly ashes) correlated with higher total REE levels. (B) High calcium content indicated greater extractability via $HNO_3$. The coal sources were Appalachian (App), Illinois Basin (IL), Powder River Basin (PRB), a, IL-PRB blend, San Juan basin, Gulf Coast, and the Highveld/Witbank coal fields in South Africa (RSA). (Taggart et al. 2016)

**Table 2.1.** REE contents and other characteristics for coal ash samples selected for Phase 1 analysis. Most fly ash samples were collected from the hopper of electrostatic precipitators (ESP), unless noted otherwise.

| Sample ID # | Power Utility (Location) | Type | Feed Coal Source | Sampling Date | Total lanthanides (mg $kg^{-1}$) | Total REE: (Lanthanides + Y +Sc) (mg $kg^{-1}$) | Specific surface area ($m^2$ $g^{-1}$) | Crystalline minerals via XRD | | |
|---|---|---|---|---|---|---|---|---|---|---|
| | | | | | | | | Major | Minor | Trace |
| 93932 | Power plant W (South Carolina) | Fly ash ESP | Appalachian | 2014 | 519 | 669 | 2.786 | Quartz | Mullite, Hematite | Magnetite? |
| 93938 | Power Plant I (Kentucky) | Fly ash - silo | Appalachian | 2014 | 570 | 703 | 7.781 | Quartz | Mullite, Hematite, Gypsum | $Ca_5(SiO_4)_2F_2$ |
| 93962 | Power Plant KS (Kentucky) | Stoker ash | Appalachian | 2015 | 961 | 1222 | 3.104 | Mullite, Quartz | Cristobalite, Hematite | Magnetite? |
| 93965 | Power Plant C (Kentucky) | Pond ash | Appalachian | 2015 | 422 | 531 | 15.10 | Quartz | Mullite, Hematite | |
| 93963 | Power Plant H, Unit 2 (Kentucky) | Fly ash - ESP | Appalachian | 2015 | 511 | 655 | 3.171 | Quartz | Mullite, Hematite | Magnetite |
| 93895 | Power Plant H (Kentucky) | Fly ash, ESP row 2 | Illinois | 2013 | 422 | 553 | 1.387 | Quartz, Magnetite | Mullite, Hematite | |
| 93899 | Power Plant H (Kentucky) | Fly ash, ESP row 3 | Illinois | 2013 | 306 | 388 | 3.661 | Quartz | Mullite, Hematite, Magnetite, Anhydrite, Calcite, Portlandite | |
| 93964 | Power Plant H, Unit 3 (Kentucky) | Fly ash, ESP | Illinois | 2015 | 408 | 524 | 1.492 | Quartz | Mullite, Hematite, Magnetite | |
| 93966 | Power Plant DE (Texas) | Fly ash, ESP | Powder River | 2015 | 332 | 406 | 1.434 | Quartz | Hematite, Periclase | Anhydrite |
| 93973 | Power Plant SC (GA) | Fly ash | Powder River | 2015 | 309 | 383 | 1.099 | Quartz | Anhydrite, Hematite, Periclase | Lime |
| 93927 | Power Plant LA (Missouri) | Fly ash | Powder River | 2013 | 211 | 265 | 1.216 | Quartz, Tricalcium aluminate, Periclase | Anhydrite, Lime | |
| 93971 | Power Plant RI | Fly ash | Powder River | 2015 | 180 | 233 | 2.451 | Quartz | Anhydrite, Lime, Tricalcium Aluminate, Periclase, Ye'elimite | Fluoroapatite, Sodalite-Nosean?, $Ca_{10}Al_{12}Cl_2Si_5O_{37}$? |

From this previous analysis, we selected 12 coal ash samples from 9 coal fired power plants for further characterization for Phase 1 of this project (Table 2.1). These samples represent ashes generated from coals of the 3 major coal-producing regions and correspond to more than 80% of annual coal ash production (approximately 100 milllion tons or more). For the samples listed in Table 2.1, we acquired more than1 to 5 kg of material per power plant for Phase 1 of this work. For Phase 2, we have already received an additional 50 gallons (approximately 200 kg) of fly ash each from Power Plants I and DE. These samples represent Appalachian-based and Powder River-based CCRs, respectively.

### 2.2 Characterization Results

Details for characterization methods have been provided in our previously published work (Taggart et al. 2016, King et al. 2018). In brief, total REE content was quantified by heated hydrofluoric/nitric acid ($HF/HNO_3$) digestion followed by analysis with inductively couple plasma mass spectrometry (Agilent 7900 ICP-MS) configured in helium reaction cell mode for removal of polyatomic interferences (Taggart et al. 2016). Our results showed that the total REE contents (defined as the sum of the lanthanides, yttrium, and scandium) were in the range of 370 to 1180 mg $kg^{-1}$.

The major element analysis, as determined by X-ray fluorescence spectroscopy, indicated patterns that were expected of coal ash of these origins. Ashes from Powder River Basin coals were characterized by the high calcium content (20-30% CaO) relative to the other samples (1-5% CaO). Illinois Basin-based ashes comprised greater iron content (20-24% $Fe_2O_3$) relative to the others (<15% $Fe_2O_3$). Silicon and aluminum were the other major metal elements and the sums of these were greater in Appalachian-based CCR samples than in samples of Illinois and Powder River origin. The dominant phase in all of the ashes is amorphous glass that could not be differentiated by X-ray diffraction. Aside from this dominant phase, the mineralogy of crystalline phases is primarily quartz in all samples as well as minor constituents. Optical and electron microscopy demonstrated the presence of distinct mineral REE-bearing phases as well as diffuse distributions of REEs in aluminosilicate glasses and amorphous carbon coatings on glass sphere.

## 3. REE Leaching from CCRs

### 3.1 Background and Objectives

As noted above, the acid extractability of REEs from fly ash depended on major characteristics of the fly ash, notably the origin of the feed coal. Fly ashes produced from Powder River Basin (PRB) coals tends to leach REEs more efficiently in $HNO_3$ compared to fly ashes from Appalachian and Illinoi Basin coals (Figure 2.1B). Moreover, our analysis of the REE speciation in fly ashes revealed a few modes of occurrence, including dispersion of REEs within aluminosilicate glass particles that make up the bulk of fly ash. Thus, our development of REE leaching strategies focused on sintering methods capable of dissolving aluminosilicate glasses. This approach entails heating the ash with an alkaline flux agent (e.g., $Na_2O_2$, NaOH, CaO,

$Na_2CO_3)_2$, $CaSO_4$, or $(NH_4)_2SO_4$) under high temperatures (300 – 450 °C). The flux reagent decomposes aluminosilicates into secondary minerals that can readily dissolve in acid at room temperature. This process has been used in the recovery of aluminum from fly ash, but has not been extensively tested for recovery of REEs. The goals of our study in Phase 1 were to compare these alkaline flux agents for their REE leaching efficiency as well as compare other process parameters (e.g. heating temperature, flux mass:ash ratio, and acid concentration) on REE leaching efficiencies. In addition to the alkaline roasting experiments, we also performed HCl acid leaching (no roasting) as a means of comparing REE extraction efficiencies between the different CCRs selected for Phase 1 work. The overall objective was to identify leaching process parameters that can yield the best REE extraction efficiencies while also minimizing costs (e.g., chemical costs, energy inputs).

### 3.2 Materials and Methods

**Coal Combustion Residue Samples.** All 12 samples shown in Table 2.1 were tested for REE recovery efficiency by HCl extraction. For the alkaline roasting method, a selection of the CCR samples (denoted in red in Table 2.1) were selected for testing. We also tested the National Institute of Standards and Technology (NIST) standard reference material (SRM) for fly ash, SRM 1633c, in leaching experiments. SRM 1633c fly ash (generated from an Appalachian-based coal feed stock) was tested mainly to verify our analysis methods, and not necessarily as a feedstock source upon scale-up (supplies of 1633c are the limited). Collectively, these ash samples were selected for their REE content (minimum of 400 mg $kg^{-1}$), geological origin (three primary U.S. coal basins represented), and ash type (stoker ash, ESP ash, silo ash, and pond ash).

**Materials.** Trace-grade acids and Milli-Q water (>18 MΩ-cm, EMD Millipore) were used for all digestions, leaching procedures, and analyses. Zirconium crucibles (5 mL and 100 mL, ESP Chemicals) were used for all sintering experiments. Samples were leached and stored in 50 mL polypropylene tubes prior to analysis and diluted using Milli-Q water and trace-grade acids. Sodium peroxide (95%) and calcium oxide (reagent grade) were purchased from Alfa Aesar. Sodium hydroxide powder (97%, reagent grade) was purchased from Sigma Aldrich. Anhydrous sodium carbonate (proteomics grade) was purchased from VWR Life Sciences. Calcium sulfate dihydrate powder (100.0% Analytical Reagent grade), ammonium sulfate (99.5% Analytical Reagent grade), and sodium hydroxide pellets (99% ACS Analytical Reagent grade) were purchased from Mallinckrodt Chemicals.

**Chemical Analysis Methods.** Total REE content in each fly ash sample was assessed previously (Taggart et al. 2016). In summary, this total REE analysis entailed overnight heated digestion of samples in a 1:1: mixture of HF:$HNO_3$. After this digestion, samples were dried and re-dissolved in dilute $HNO_3$ for analysis by inductively coupled mass spectrometry (ICP-MS) on an Agilent 7900 configured with He- and $H_2$-reaction gas collision cell for interference removal. Recovery of certified element contents for the NIST SRM 1633c fly ash was used to validate the HF/$HNO_3$ digestion approach. Recoveries were approximately 95% of the certified values for REEs (Taggart et al. 2016).

**Alkaline Roasting and Acid Extraction of REEs.** Sodium peroxide ($Na_2O_2$) alkaline sintering (as described by the U.S. Geological Survey (Lichte et al. 1987, Meier and Slowik 1994, Meier et al. 1996)) has been used as a method for quantifying total REE contents in fly ash. Thus, this approach served as the baseline for our extraction technique, and reaction parameters were systematically altered from this baseline approach. Ash samples (0.1 g) were placed into 5 mL zirconium crucibles, mixed with $Na_2O_2$ (0.6 g), and heated at 450°C for 30 minutes. After cooling, the crucibles and their contents were submerged overnight in 20 mL of Milli-Q water. The next day, the crucibles were removed using forceps and carefully rinsed into the solution using 20 mL of 25% v/v $HNO_3$. An additional 10 mL of MilliQ water was added to dilute the samples to 50 mL (for a final $HNO_3$ concentration of 2 M) for storage and ICP-MS analysis.

Further extraction experiments entailed modification of this same basic procedure with the alkaline flux type, flux-ash ratio, acid leach strength, and temperature. Flux types were compared initially using the previously outlined method (0.6 g of flux, 0.1 g of ash, roasted at 450°C for 30 minutes and leached with 20 mL of Milli-Q water followed by 20 mL of 25% v/v $HNO_3$) to achieve a final leach acid concentration of 2 M. The tested flux agents were CaO, $Na_2CO_3$, $CaSO_4$, $(NH_4)_2SO_4$, and NaOH. The effect of decreasing the flux-to-ash ratio was tested for CaO, $Na_2CO_3$, NaOH, and $Na_2O_2$ by using only 0.1 g of flux per 0.1 g of ash (parity) rather than the previous 0.6 g of flux per 0.1 g ash (a 6:1 excess). All other conditions (temperature, duration, leaching solutions) were held constant at the previously outlined values.

The NaOH flux yielded promising results; thus, further experiments evaluated the importance of roasting temperature. This entailed experiments with 0.1 g of ash and 0.1 g of NaOH, sintered for 30 minutes, leached with 20 mL of Milli-Q water, and acidified the next day with 20 mL of 1 M $HNO_3$. The sinters were identical except for the sintering temperatures, which were 450°C, 350°C, 250°C, and 150°C.

The recovery of REEs in all CCR samples was also attempted via acid leaching (no alkaline roasting). In these tests, 1 g of CCR sample was combined with 10 mL of HCl (at concentration of 12 M or 6 M) and heated on a hotblock to 85 °C for 4 h. Another set of samples (1 g each) was also mixed with 1M HCl or 1M $HNO_3$, rotated end-over-end for 24 h at room temperature (22-23°C). After the defined leaching time, the solids were allowed to settle for a few minutes and then an aliquot of the overlying supernatant (typically 100 μL) was diluted into 10 mL of 2%$HNO_3$/0.5%HCl (v/v) for preservation and later analysis via ICP-MS.

### 3.3 Results and Discussion

The sinter with sodium peroxide ($Na_2O_2$) resulted in 55-110% extraction of REEs from the coal ash samples (Figure 3.1), where the total REE content was defined by extraction with heated HF/$HNO_3$ digestion. Other flux materials were also tested, as they were expected to be less expensive than and more readily available alternatives to $Na_2O_2$. Of all the fluxes tested, NaOH performed the best, with average REE recovery superior to the $Na_2O_2$ method in some cases. Lime (CaO) and soda ($Na_2CO_3$) sinters were found to be ineffective (generally less than

40% recovery) (Figure 3.1). We hypothesize that this is due to the melting temperatures for these compounds (>700 °C for CaO, $Na_2CO_3$, $CaSO_4$) that were greater than the roasting temperature that we tested for the sinter (450°C). Sulfate compounds (calcium and ammonium sulfate) likewise had poor REE recovery. In the case of ammonium sulfate, this may have been due to insufficient sintering time (only 30 minutes) or insufficient alkalinity rather than the temperature ($NH_4SO_4$ melting point is 455°C).

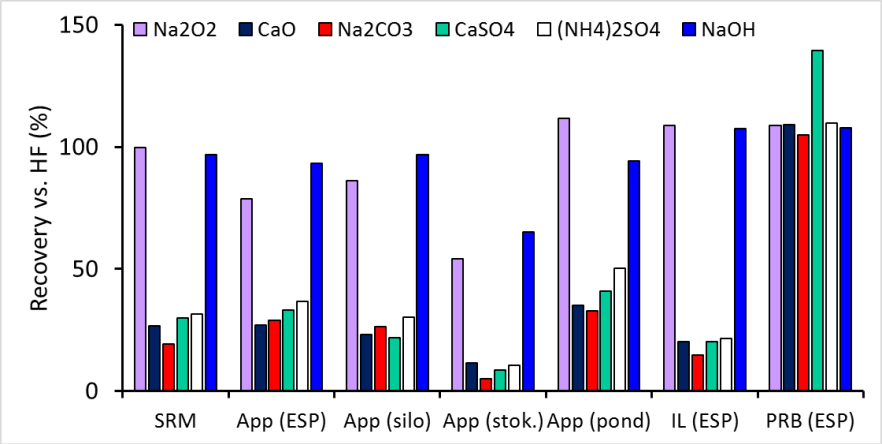


**Figure 3.1.** Recovery of REEs (relative to total REEs as determined by $HF/HNO_3$ acid digestion) for fly ash samples subjected to alkaline sintering followed by $HNO_3$ leaching. In all experiments, 0.1 g of fly ash was mixed with 0.6 g of alkaline flux (noted in the figure legend), heated for 30 min at 450°C, and subsequently leached in water and 2M $HNO_3$.

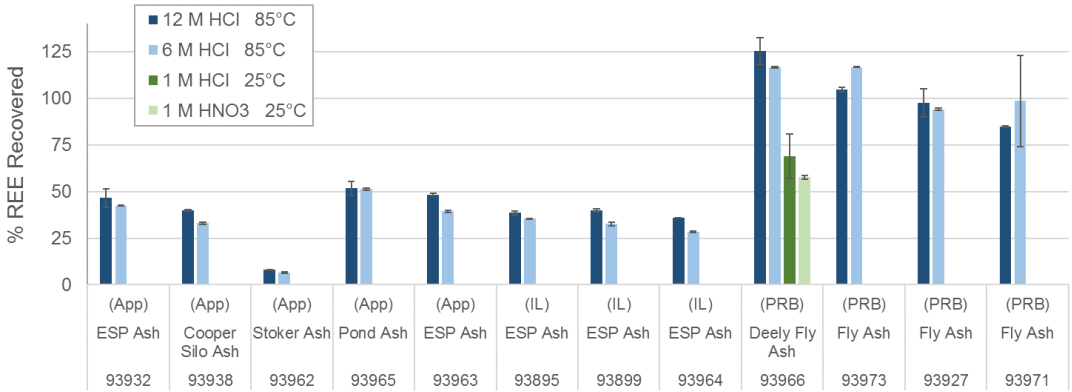


**Figure 3.2.** Recovery of REEs (relative to total REE as determined by $HF/HNO_3$ acid digestion) for CCR samples subjected acid leaching (no alkaline roasting). Relatively high recoveries of REEs were observed with the PRB fly ash samples compared to the Appalachian Basin and Illinois Basin coal ashes.

For the PRB fly ash, the recovery of REEs was notably close to 100% for all flux agents (Figure 3.1). We believe this is because the final $HNO_3$ leaching step was effective for leaching REEs from this sample. In our tests of REE leaching with HCl and $HNO_3$ (Figure 3.2), we observed >75% recovery of REEs from the PRB-based fly ash samples during heated acid extraction, while the Appalachian- and Illinois-based CCRs resulted in less than 50% recovered by heated acid extraction. These results suggest that the alkaline roasting step was not needed for

recovery of REEs from the PRB fly ash.

The stoker ash was the sample with the greatest total REE content (1222 mg $kg^{-1}$). However, REE recoveries for this sample were noticeably lower than for all other samples. Even the most successful sinter methods, including the sodium peroxide, failed to recover more than about 50% of the total REE. This result could be explained by the vastly different appearance and much larger grain size of the stoker ash. The stoker ash has a consistency that is more skin to bottom ash, and likely comprises more unburned carbon than fly ash.

We also examined other elements for their extraction efficiency, mainly to identify potentially toxic metals in the final product. Fly ash can be enriched in naturally occurring radioactive materials that are the decay products of thorium (Th) and uranium (U) (Lauer et al. 2015). Thus, co-extraction of these elements with the REEs could result in challenges with radioactivity as the REEs are further concentrated in downstream recovery processes.

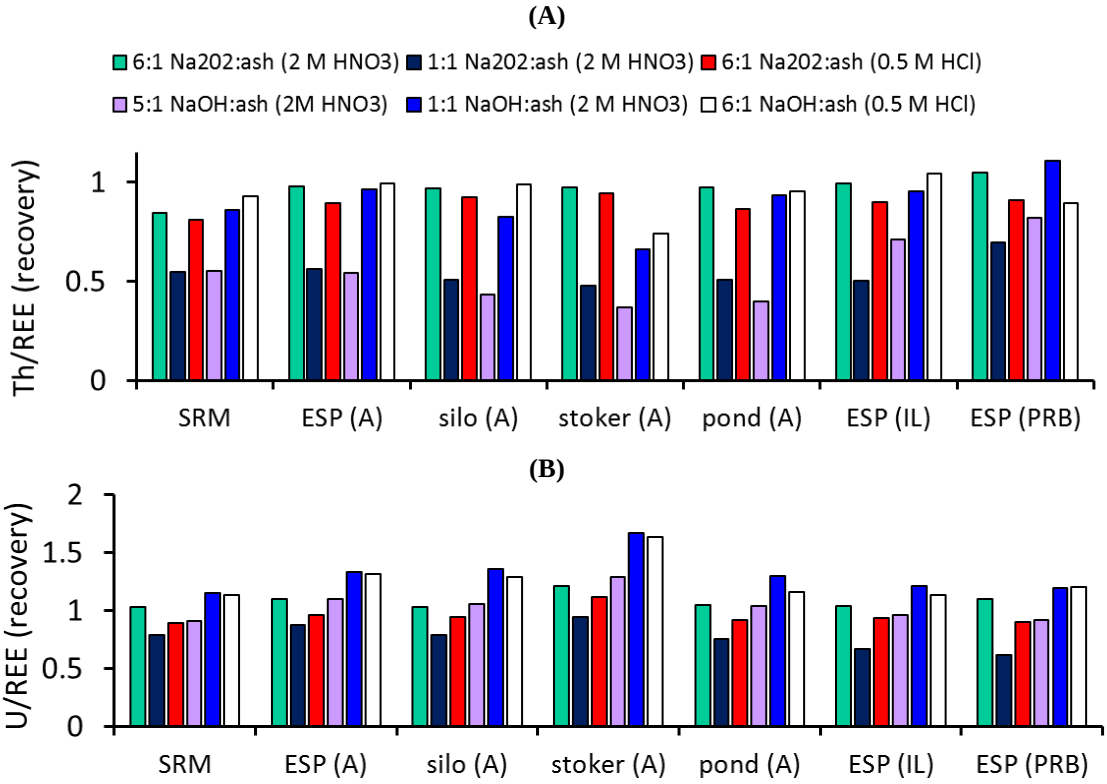


**Figure 3.3.** (A) Fraction of thorium (Th) leached into solution relative to the fraction of total REEs leached into solution after alkaline sintering. (B) Fraction of uranium (U) relative to the fraction of REEs leached. Ratios less than 1 denote differential partitioning of the trace element relative to the REEs, while ratios equal to 1 suggest that the trace element is leaching to a similar extent as the REEs and could become enriched in the final product as REEs are enriched.

For the alkaline sintering process, we observed that Th and U were also leached with the REEs, but the recovery of these elements varied considerably. The relative recovery of Th was generally less than the relative recovery of REEs. In other words, as shown in Figure 3.3A, the recovered fraction of Th normalized to the recovered fraction of REEs was less than 1 in many cases, suggesting that the leaching process resulted in dilution of Th between process streams

whereas REEs were mostly partitioning to the acid leachate stream (for the NaOH flux). Uranium was showing different trends in that this element seemed to track with the REEs in the leaching process (relative ratio of U recoverd/REE recovered was equal to 1) (Figure 3.3B).

Due to the success of the initial NaOH sinter, subsequent extractions were performed with less mass of flux reagent and more dilute $HNO_3$ leachate solution. The use of less flux mass also decreased the loading of sodium to downstream separation and purification processes. Results of this experiment demonstrated REE recoveries of 75% or greater when using equal parts ash and flux and 2 M $HNO_3$ for the acid leaching step (blue bars in Figure 3.4). Roasting temperature also influenced recovery efficiencies. For the NaOH sinter, roasting at 350°C and 450°C yielded similar recoveries while roasting at lower temperatures (150°C and 250°C) resulted in much lower recovery. This result is consistent with the hypothesis that roasting needs to exceed the melting temperature of the flux agent (318°C for NaOH). Recoveries were similar with 2 M $HNO_3$ but decreased with acid leaching strengths at $HNO_3$ concentrations of 0.1 M and less (Figure 3.5). Overall, these results suggest that NaOH is an ideal candidate for replacing sodium peroxide for scalable, sinter-based REE extraction methods targeting coal fly ash.

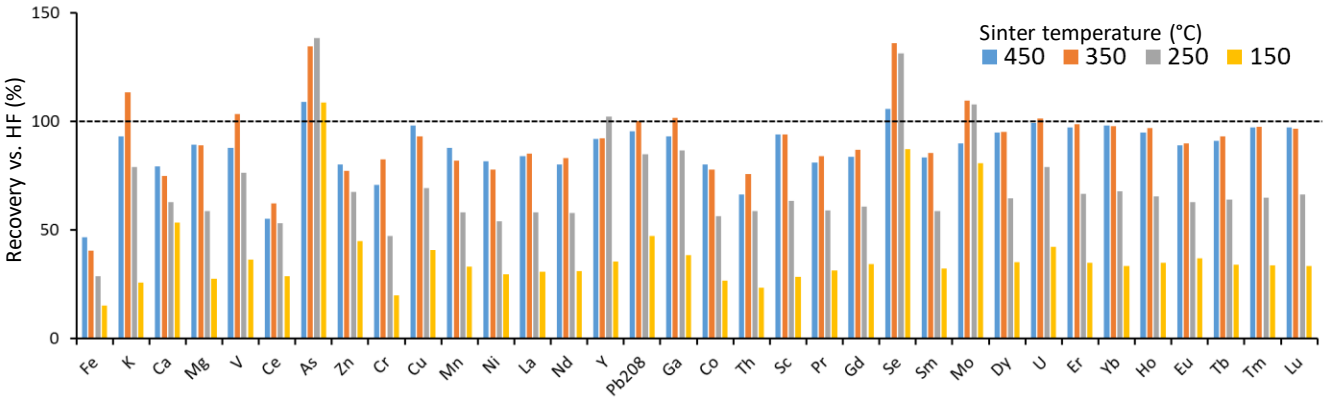


**Figure 3.4.** Recovery of major and trace elements after roasting an Appalachian fly ash (Kentucky Cooper Station silo fly ash) with NaOH (1:1 mass ratio) at variable temperatures for 30 minutes, followed by acid leaching with $HNO_3$.

Overall, our testing suggests that our bench-scale system should focus on the following chemical extraction methods for REEs from coal ash:

- Dilute acid extraction with heated $HNO_3$ or HCl for PRB-based coal fly ash
- For Appalachian and Illinois Basin coal fly ash, pretreatment with alkaline sintering is necessary.
- Alkaline sintering can involve NaOH (1:1 mass ratio with ash) heated to >350°C for 30 minutes.
- Acid leaching following sintering should utilize strong acid ($HNO_3$ or HCl) with a concentration of 0.1M to 1 M (depending on NaOH mass), to achieve a pH value in the range of 0 to 3.

These process parameters listed above were the main conditions used to generate feedstock for downstream membrane separation processes.

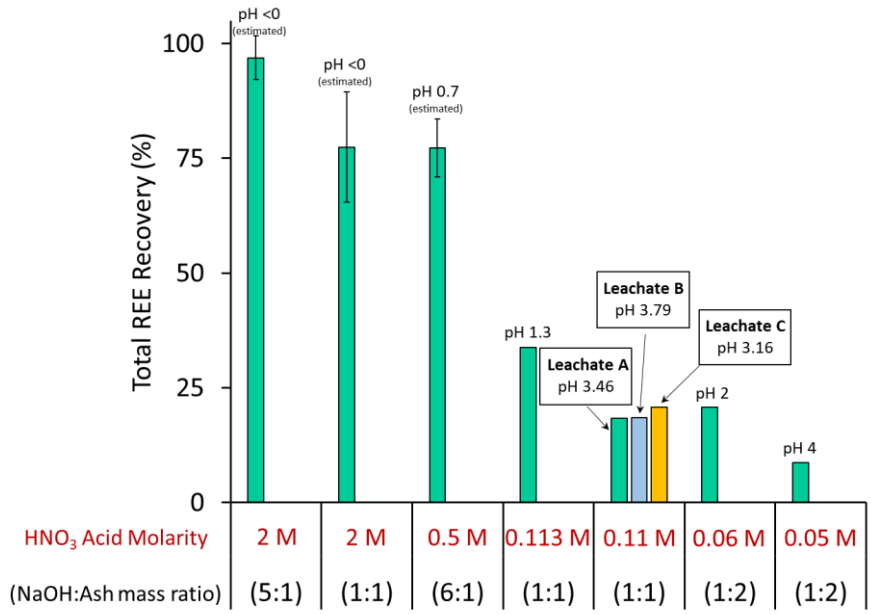


**Figure 3.5.** Recovery of total REEs from the Cooper Station silo fly ash that was processed by NaOH roasting (450°C) followed by acid leaching with nitric acid ($HNO_3$). Results demonstrated variable extraction efficiencies depending on the relative amount of NaOH during the roasting step and the $HNO_3$ leach strength. The pH values correspond to the estimated or measured pH at the end of the overnight extraction period. Error bars denote one standard deviation of triplicate extractions, where available. Replicate Leachates A, B, and C are plotted separately because they were used for a variety of downstream liquid membrane separations in later sections.

## 4. Micelle-Enhanced Ultrafiltration

### 4.1 Background and Objectives

Micelle-enhanced ultrafiltration (MEUF) is a metal ion separation method that was tested for REE recovery from coal ash leachates. MEUF separations involves the addition of a surfactant (sodium dodecyl sulfate) to the coal ash leachate, resulting in micelles that sorb metal cations such as REEs. The REE-encapsulated micelles can then be separated from dissolved ions by ultrafiltration. This method was first tested on a synthetic test solution of mixed REEs and then later tested on an HCl acid leachate of fly ash from Plant DE (PRB-based ash).

### 4.2 Materials and Methods

The synthetic test solution comprised of six elements (Tb, Nd, Y, Eu, Er, and Dy), each added as nitrate salts to a concentration of 12 mg $L^{-1}$ in deionized water. Sodium dodecyl sulfate (SDS) was added to this mixture to achieve a final concentration of 0.5 to 11 mM. Another set of MEUF separations was performed with a filtered (<0.45-μm) acid extract of the PRB Plant DE fly ash. This acid extract was generated by heated HCl extraction in 6 M HCl (as described in Section 3 and leaching results shown in Figure 3.2). A single SDS concentration (8 mM) was tested for this mixture. This concentration value was selected based on experiments with the synthetic REE solution.

Upon addition of SDS to the test mixture and fly ash acid leachate, micelles formed immediately. The mixtures were stirred at 150 rpm at room temperature for 60 min to allow metal cations to sorb to the micelles. The mixture was then separated by a UP020 ultrafiltration membrane at 3 bar pressure for recovery of micelles in the rentate. REE content of the retentate was quantified by digesting the retentate in heated nitric acid and analysis of the digestion solution with ICP-MS.

### 4.3 Results and Discussion

***Micelle-Enhanced Ultrafiltration*.** Our initial testing of the MEUF process demonstrated that REEs could be concentrated from relatively pure solutions of mixed REEs (Figure 4.1A). The recoveries depended on the SDS concentration as well as other process conditions. However, for the acid leachate of a fly ash sample, REE recovery was suboptimal (less than 20% recovered in the MEUF retentate) (Figure 4.1B). The low recovery of REEs from the fly ash leachate could be due to the presence of other major ions such as Al, Si, Ca, and Fe that interfered with the sorption of REEs to the SDS micelles. Thus, we concluded that MEUF was not adequately selective for REEs and did not pursue this method any further.

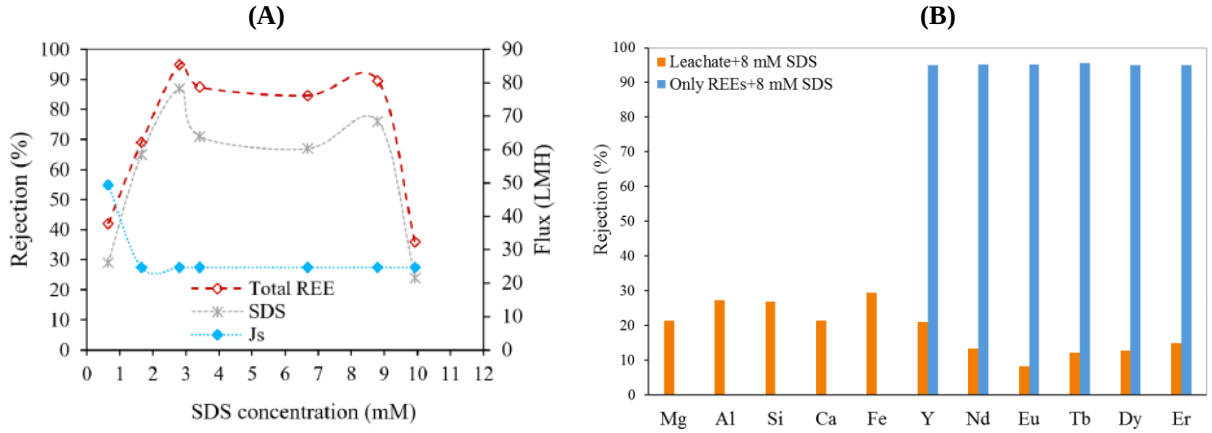


**Figure 4.1.** (A) Recovery of REEs by micelle-enhanced ultrafiltration from a synthetic solution of Tb, Nd, Y, Eu, Er, and Dy (12 mg $L^{-1}$ each) in deionized water. A range of sodium dodecyl sulfate (SDS) concentrations did not appear to alter the flux across the membrane, but altered the recoverable fraction of REEs. (B) Recoveries of REEs from an acid leachate of the Plant DE fly ash (PRB coal source) were substantially lower than recoveries from the synthetic test solution comprising only REEs. The presence of other major ions in the fly ash leachate was a major interference for REEs.

## 5. Liquid Emulsion Membranes, Supported Liquid Membranes

### 5.1 Background and Objectives

Liquid emulsion membranes (LEM) and supported liquid membranes (SLM) are liquid membrane methods that have been used for recovery of REEs and other metal cations from aqueous mixtures (Bartsch and Way 1996, Kulkarni et al. 2002, Gaikwad et al. 2003, Kocherginsky et al. 2007, Hasan et al. 2009, Kim et al. 2015). Here we compared LEM and SLM for REE extraction efficiencies from acid leachates of coal fly ash. Both LEM and SLM are

conceptually similar to conventional solvent extraction methods for recovery of REEs from acid streams. Both utilize a hydrophobic REE extractant (i.e. metal chelator) dissolved in an organic solvent (such as kerosene) as a means to selectively partition REEs from other metals in the feed solution. LEM and SLM are unique to the conventional approach in their configurations, which aim to maximize interfacial contact area between the aqueous feed, organic solvent, and acid stripping reagent. These configurations enable a reduction in the use of chemicals (solvent, extractant, acids) that would be cost drivers of conventional solvent extraction.

For Phase 1, we tested the efficiencies of LEM and SLM processes for recovery of REEs from coal ash leachates. The separations focused on process parameters such as pH of the coal ash leachate feed solution (pH 1 – 4) and extraction time. We also compared separation efficiencies using either kerosene or mineral oil as the solvent for the liquid membrane. The rationale for these two solvents was that kerosene is commonly used for solvent extraction processes, including REE separations, while mineral oil would be a less hazardous alternative to kerosene.

### 5.2 Materials and Methods

***Materials.*** Trace-grade nitric acid (99.999% purity) and Milli-Q water (>18 MΩ-cm, EMD Millipore) were used to make reagents for all experiments. The metal chelating agent 97% di-(ethylhexyl) phosphoric acid (DEHPA), organic solvents kerosene (purum) and mineral oil, and surfactant Span 80 were all purchased from Sigma Aldrich and used without further purification.

Initial proof-of-concept testing was performed with a synthetic solution based on the known ion composition of acid leachate solutions. This synthetic solution comprised major cations ($Na^+$, $Mg^{2+}$, $Al^{3+}$, $Ca^{2+}$, $Fe^{2+}$) added as nitrate salts, Si as $Na_2SiO_3$, and 7 individual REEs ($Sc^{3+}$, $Y^{3+}$, $Nd^{3+}$, $Eu^{3+}$, $Tb^{3+}$, $Dy^{3+}$, and $Er^{3+}$) added as nitrate salts to Milli-Q water containing dilute $HNO_3$. This synthetic mixture was used in initial experiments as a means to provide a consistent feed solution as we compared multiple types of REE recovery methods (e.g. liquid membranes, nanofiltration, electrodeposition, etc.), particularly as we were simultaneously developing the alkaline roasting method for extraction of REEs from fly ash.

Subsequent SLM and LEM experiments utilized real acid leachate of silo fly ash from Plant I (Cooper Station, KY). Leaching was accomplished by mixing 4 g silo fly ash with 4 g powdered NaOH and roasting at 450 °C for 30 mins. After the roasting step, the mixture was leached in 0.11 M $HNO_3$ for 12 hrs. The supernatant was decanted from any settled solids and used without further modification..

***Liquid Emulsion Membrane (LEM).*** The LEM process entails the formation of an emulsion with nitric acid and an oil phase containing DEHPA. The oil-phase of the emulsion was prepared by combining either kerosene or mineral oil with Span 80 and DEHPA to a 150 mL Erlenmeyer flask and stirring until completely mixed. The ratio of oil/Span 80/DEHPA varied, but the final total volume of all organic solvents was always 50 mL. Nitric acid (50 mL of 5 M) was then added dropwise under high speed mixing at 5000 RPM (T18 Ultra-Turrax disperser,

IKA Works, Inc.) to bring the total volume of the prepared emulsion to 100 mL.

This emulsion was added to 500 mL of coal ash leachate (both synthetic and real leachates) and stirred for 30 min (100-200 RPM). The leachate/emulsion mixture was then poured into a 2 L glass separatory funnel, held static for 2 hours, and then manually decanted into separate aqueous and emulsion phases. Demulsification was achieved by either heating at 60 to 70 °C or by letting the mixture naturally separate into two phases over a period of 48 hrs. The concentration of major and minor metals, including the REEs, were quantified in the acid stripping phase via ICP-MS. Initial proof-of-concept testing of the LEM system was performed using synthetic coal ash leachate. After this initial testing, LEM separations were performed on real fly ash leachate (Leachate C).

***Supported Liquid Membrane (SLM).*** SLM used a similar process except that the organic solvent was loaded on a hydrophobic membrane. In this configuration REEs from the coal ash leachate on the feed side of the membrane partition through the organic solvent layer of the liquid membrane and concentrate on the product side in the $HNO_3$ stripping solution. SLM often uses a hollow fiber membrane module, which are commercially available. Moreover, SLM has been tested at the demonstration scale for recovery of REEs from electronic wastes (Kim et al. 2015), but has not been tested for coal ash leachates.

For all experiments, a 47-mm PVDF membrane with 0.22-µm nominal pore size (EMD Millipore) was impregnated with a 10% (v/v) DEHPA solution in either kerosene or mineral oil. The DEHPA solution was pulled through the membrane using a vacuum filtration apparatus. The filter was then placed in a shallow bath of the DEHPA solution and allowed to soak for at least 2 hours. SLM separations were performed on a two chamber H-cell (Adams & Chittenden Scientific Glass, Berkeley, CA) consisting of two 250 mL glass media bottles with flanges that allowed a 47 mm membrane to be inserted between the two bottles. One side of the reactor was filled with 250 mL of ash leachate while the other side contained the stripping solution (5 M $HNO_3$). Both chambers were continuously mixed using stir bars. Samples were collected periodically from the feed and stripping phases for up to 24 hours, and major and minor metal elements were quantified by ICP-MS. In one experiment, the metals content in the membrane after a 24 h SLM separation with a fly ash leachate was quantified by ashing the membrane at 550°C for 2 h and then heated acid digestion of the ashed membrane in concentrated $HNO_3$. After digestion, the sample was diluted with deionized water and REE contents were quantified by ICP-MS.

Initial tests with SLM separations utilized the synthetic coal ash leachate, and subsequent tests were performed on Leachates A and B generated from Plant I silo fly ash. Leachate A was used as the feed for a single SLM separation, while Leachate B was used for two SLM separations in series. For this two-stage system, Leachate B was subjected to 24 h separation via SLM. The 5 M $HNO_3$ acid product from this first stage was neutralized to pH 3 using powdered NaOH and then used as the feed for another 24 hr SLM separation process (Stage 2). REE content and major cations were quantified in the original Leachate B feed and product solutions

of Stage 1 and Stage 2.

***Chemical Precipitation and Nanofiltration.*** Results of the LEM and SLM separations demonstrated promising results in recovering REEs from coal ash leachates. However, the presence of major ions such as $Fe^{3+}$, $Al^{3+}$, $Si^{4+}$ and $Na^{+}$ were limiting the REE purity of the final product. Thus, additional separations were explored as 'clean-up' steps of the feed or production solutions for the liquid membrane separations. These additional steps included chemical precipitation of major metal oxides by adjusting the pH of the mixture with NaOH, allowing the mixture to precipitate for 90 minutes, and then removal of particles by a 0.45 μm nitrocellulose filter. This process was explored as a means to remove $Fe^{3+}$, $Al^{3+}$, $Si^{4+}$ from REE concentrates.

Another clean-up step involved nanofiltration, which can separate multivalent ions (e.g. REEs) from monovalent ions (e.g., $Na^{+}$). We tested two hydrophilic polyethersufone membranes, NP010 (MicroDyn-Nadir) and NP030 (MicroDyn-Nadir), and two polymeric thin-film membranes, DK (GE Osmonics), Duracid (GE Osmonics) (Table 5.1), all run at 24 bar pressure in a cross-low flat sheet stainless steel filtration apparatus with a 155 $cm^2$ membrane surface area. REE contents were quantified in the NF retentate via ICP-MS. Both chemical precipitation and NF separations were tested on the synthetic solution.

**Table 5.1.** Manufacturer specifications for nanofiltration membranes tested for synthetic coal ash leachates.

| | **NP010** | **NP030** | **DK** | **Duracid** |
|---|---|---|---|---|
| Manufacturer | Microdyn-Nadir | | GE W&P Technologies | |
| Polymer | Permanently hydrophilic PES | | Thin film composite [(a)] | |
| $P_{max}$ (bar) | 40 | 40 | 40 | 60 |
| $T_{max}$ (°C) | 95 | 95 | 50 | 70 |
| pH range | 0-14 | 0-14 | 1-10 | 0-9 |
| MWCO (Dalton) | ~1000 | ~500 | ~150-300 | ~150-200 |
| Pure water flux (L $h^{-1}$ $m^{-2}$ $bar^{-1}$) | 5-10 | 1-1.8 | 5.5±25% | 1.1-2.1 |
| Salt Rejection (%) | 35-75 [(b)] | 80-95 [(b)] | 96 [(c)] | 98 [(c)] |

[(a)] Poly(piperazine-amide) based interfacial polymerization membrane on a polysulfone support layer and two proprietary layers backed by a polyester support (Vandezande et al. 2008).
[(b)] Tested salt: $Na_2SO_4$; [(c)] Tested salt: $MgSO_4$.

## 5.3 Results and Discussion

***Liquid Emulsion Membranes.*** The LEM separation generally demonstrated favorable REE recoveries from both the synthetic and real fly ash leachates. For initial tests with the synthetic leachate feed, LEM separations with the kerosene solvent demonstrated enhanced recovery of Y, Nd, Eu, Tb, Dy, Er (20-60% recovered) and rejection of major ions such as Na, Al, and Fe (less than 2% recovered) (Figure 5.1). Improved recoveries were observed if this synthetic ash leachate was adjusted to pH 2.5 prior to LEM separation (Figure 5.1).

The emulsions with mineral oil instead of kerosene produced similar recovery efficiencies, and perhaps better results for REE recovery relative to the kerosene emulsions (Figure 5.1). Additionally, the amount of surfactant Span 80 present in the emulsion also affected total recovery. At high surfactant concentration (3%) recoveries were very poor with mineral oil. The lower surfactant concentrations (1%) resulted in better recoveries; however we note that the

emulsion was less stable at the 1% Span 80 concentration. Overall, these results suggest that a key optimization parameter for the LEM process is the relative amount of Span 80 in the emulsion, where the trade-offs are emulsion stability and overall REE recovery efficiency. In Phase 1, we did not have the opportunity to examine these trade-offs in detail, but decided to use 2% Span 80 for subsequent LEM separations with real fly ash leachates.

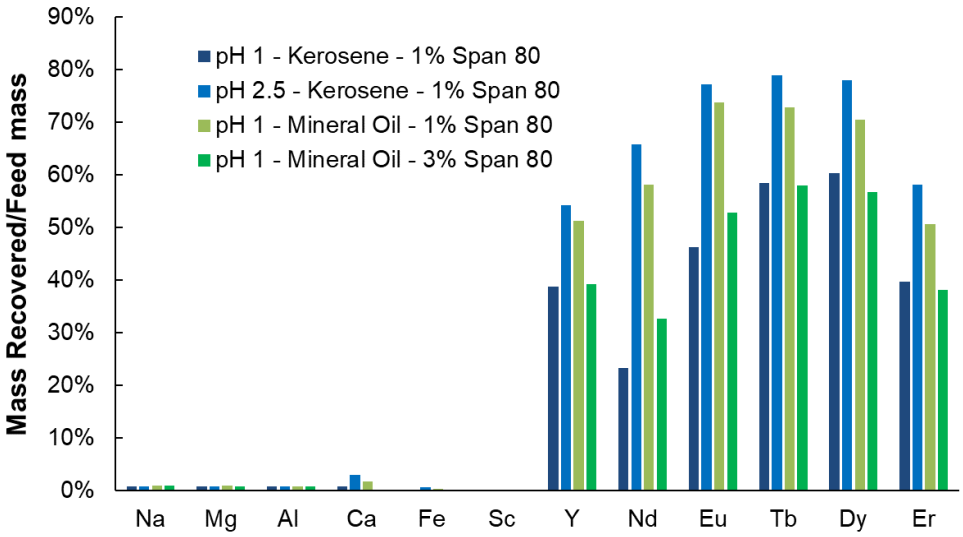


**Figure 5.1.** Recovery of selected elements from synthetic coal ash leachate subjected to liquid emulsion membrane separation. The data show results of two configurations: separation using the kerosene emulsion or the mineral oil emulsion, both using Span 80 as the surfactant for the emulsion.

In testing with real fly ash leachates, the LEM process also demonstrated promising results in concentrating and separating REEs. The recovery of REEs by LEM separation was approximately 40-75% for the more abundant REEs (Y, La, Ce, Nd) as well as other high value REEs (Eu, Dy, Er) (Figure 5.2). We also observed that $Ca^{2+}$ and $Al^{3+}$ were concentrated to a significant degree, and this likely contributed significantly to the non-REE dry mass in the LEM product.

From these results, we determined the REE content of the LEM product by estimating the dried solid weight from the measured aqueous phase composition. These calculations used the aqueous phase measurements of all major and minor cations (including the REEs) and assumed their occurrence as nitrate salts in a dry mass product. The calculation resulted in a REE content of 0.07 wt.% for the LEM product.

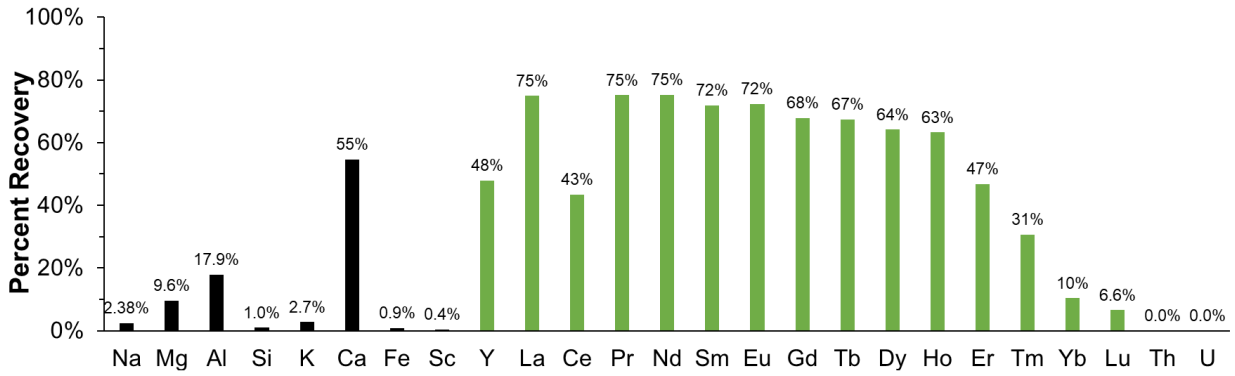


**Figure 5.2.** Recovery of selected elements from fly ash Leachate C subjected to liquid emulsion membrane separation (mineral oil, 2% Span-80).

***Supported Liquid Membranes*.** The supported liquid membrane approach follows a similar concept as the LEM approach except that the organic solvent phase is added to the pore space of a hydrophobic membrane and this membrane separates the leachate feedstock and acid stripping phase in one reaction vessel. The results of SLM testing with a synthetic coal ash leachate demonstrated enhanced recovery of selected REEs (Er, Y, Dy, Tb, Eu) and rejection of major ions such as Al, Fe, Si for both kerosene- and mineral-oil based liquid membranes (Figure 5.3), a general result that is similar to our experiments with the emulsion configuration.

The use of mineral oil resulted in slightly reduced recoveries of REEs relative to the kerosene liquid membrane (Figure 5.3B), a result that is different from the liquid emulsion approach. We believe that mineral oil might be less stable in the pores of the membrane: small amounts of mineral oil had visibly partitioned into the feed and product solutions during the 20 h separation.

A notable difference between the liquid emulsion and supported liquid membrane approaches is that the SLM method is a kinetics-based separation method while LEM (as well as conventional solvent extraction) is an equilibrium based separation. In this respect, REE separations via the support liquid membranes depend on *rate* of extraction and not simply thermodynamically-driven separations. In our testing with silo fly ash Leachate A, we observed that certain REEs extracted more quickly than others. In particular, the heavy REEs tended to extract more efficiency over a 24 h time period than the light REEs (Figure 5.4). These results suggest that SLM has advantages in extracting higher value REES (e.g., Y, Dy, Er) over the lower value and more abundant REEs (e.g., La, Ce).

**(A)** **(B)**

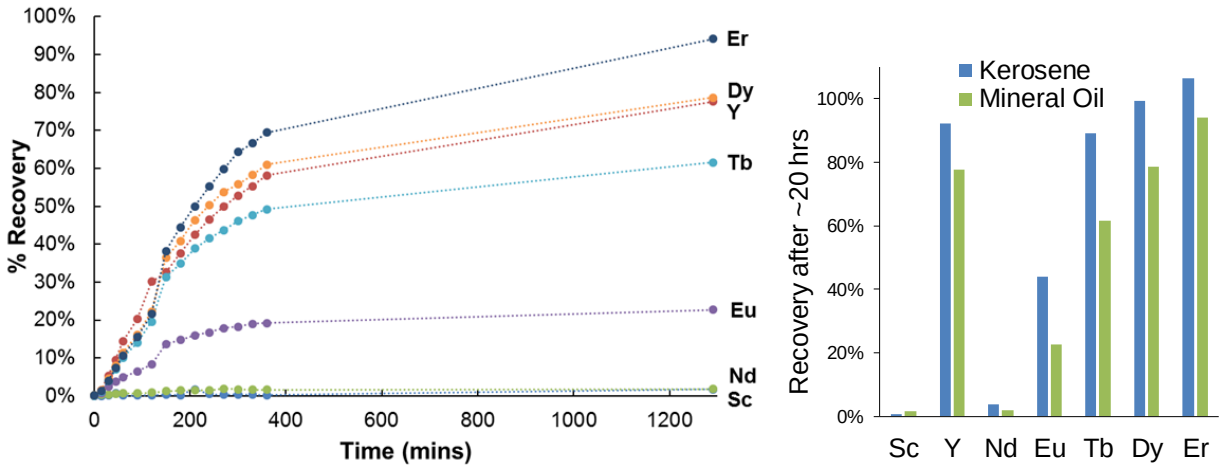


**Figure 5.3.** (A) Recovery of REEs in the supported liquid membrane configuration using mineral oil solvent in a PVDF membrane system with synthetic leachate feed. Major ions Al, Fe, and Si were less than 5% of the original in the product. (B) Comparison of kerosene and mineral oil solvents in the supported liquid membrane configurations.

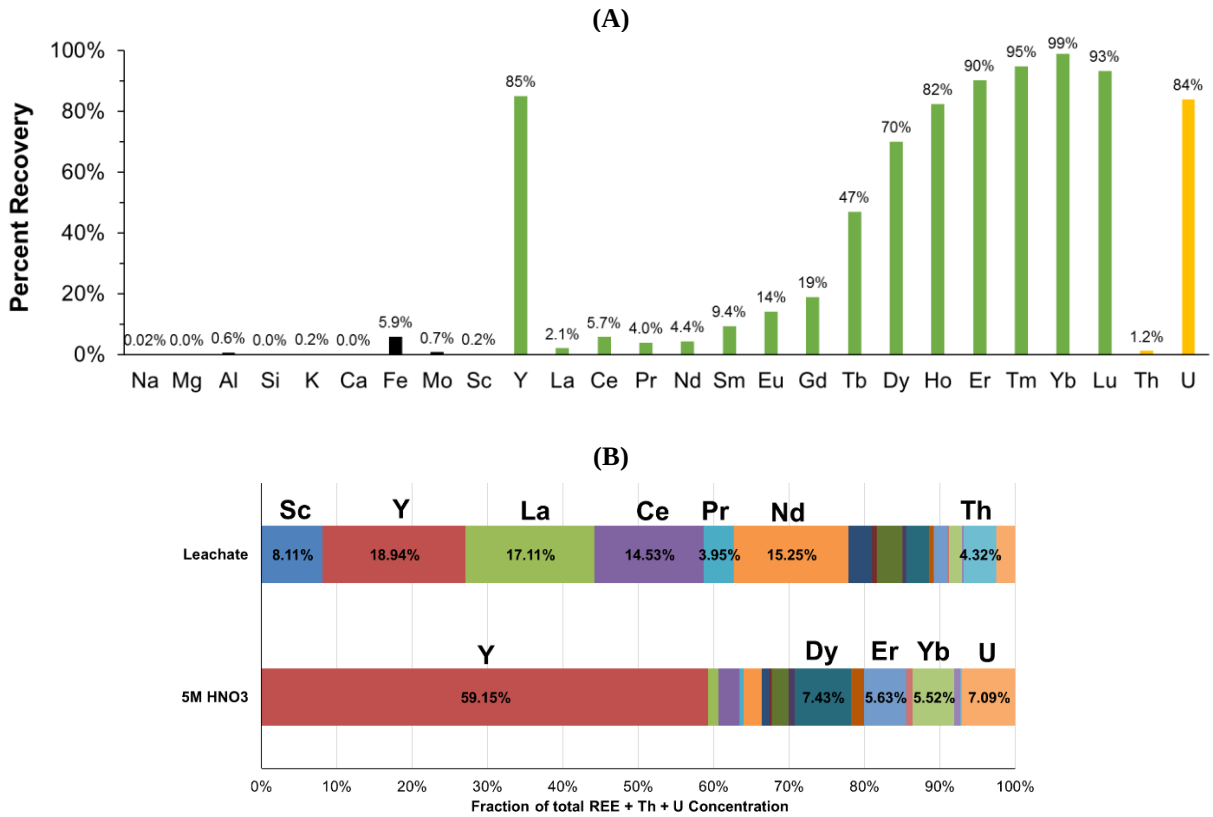


**Figure 5.4.** (A) % Recovery of REEs after 24 h in a mineral oil-based supported liquid membrane (SLM) for a feedstock comprising Leachate A shown in Figure 6 (Plant I silo fly ash, Appalachian-based). (B) Relative proportion of REEs in the fly ash leachate feed solution for SLM and in the final acid stripping product solution after SLM separation.

The REE content (dry wt%) of the SLM separation product of Leachate A was determined by two methods. First, the dry mass of the SLM product was calculated by summing all major and minor cations measured by ICP-MS in the aqueous mixture and assuming their occurrence as nitrate salts (e.g. $Fe(NO_3)_3$, $Al(NO_3)_3$, $Si(NO_3)_4$, $Ca(NO_3)_2$, $NaNO_3$, $Sc(NO_3)_3$, $Y(NO_3)_3$, $La(NO_3)_3$, $Ce(NO_3)_3$, etc.). From this basis, the REE content of this product was 1.1 wt.%. The second method of determining the REE content was to dry 20 mL of SLM product on a hot plate and quantify the mass of dried powder from this volume. This resulted in 0.3 mg of powder generated from 20 mL of volume. With the measured concentrations of REEs in that 20 mL volume, we estimated the REE content of the dried powder to be 0.97 wt%, which is close to the first method of determination.

In all SLM separations, Sc was not observed in appreciable quantities in the acid stripping product of the membrane system, but was also lost from the feed side of the SLM reactor. We examined the PVDF membrane after one SLM experiment with a silo fly ash leachate (composition not shown) that was subjected to 24 hours on the SLM reactor. This membrane contained a substantial amount of Sc, accounting for more than 75% of the total Sc in original feed solution. This result demonstrates a promising approach for a second mixed REE product that is enriched in Sc, an element with a high market price relative to the other individual REEs.

Overall, these results suggest that the SLM process was capable of separating REEs from major ions. We also note that the process also concentrated uranium, a naturally occurring radioactive element in fly ash. The calculated U content of the SLM product was 0.09 wt% (dry basis) or 900 parts-per-million. Thus, the presence of U in the final product and its implication for radioactivity will continue to be monitored in Phase 2. Thorium was not concentrated in appreciable quantities.

## 6. Electrochemical Deposition

### 6.1 Background and Objectives

Briefly, the electrochemical deposition (ED) technology utilizes electrochemically conductive filters comprised of carbon nanotubes (CNTs; multi-walled) encapsulated in a thin polymeric coating to minimize release of CNTs. These filters are assembled as multiple stacks in series such that a unique electrochemical potential can be applied to each filter, where increasing potentials are applied at subsequent stages (i.e., trapping easiest-to-reduce metals first followed by more-difficult-to-reduce metals at later stages). This results in the formation of metal or metal oxide clusters (ranging from nm to um sizes) on the surface of the filter, which we hypothesized could be mechanically recovered for direct material reuse when sufficient mass was deposited on the filter. Ultimately, the goal of the ED unit is to enable semi-continuous separation and recovery of multiple metals from mixed-metal stream by pausing the wet filtration, splaying the filter stack, recovering unique metals at each stage, and subsequently reusing the filters. In order to avoid interruption of the wet chemical stream, we envision operating (at least) dual filter stacks, enabling one to be operational while the other is offline for

the mechanical collection of solid, relatively pure REEs. Note that the ED device, in addition to functioning to separate bulk elements from REEs, may functionally serve as a "drying" step, where bulk fluids can pass the filter for potential clean up and reuse and target REEs are directly recovered as dry solids.

The objectives include optimizing the efficacy of the recovery process for a series of standard solutions over a range of pHs (2-10), flow rates (1-5 mL $min^{-1}$), and applied potentials (0-3 V) for a series of metals (Cu, Eu, Sc, Nd, and Ga) and metalloids (As). In addition to these originally proposed objectives, we also investigated the ability of the filter stack to selectively recover REEs over bulk elements in a synthetic SLM product (via ICP-MS) and qualitatively from a real CCR leachate solution (via EDX-SEM).

### 6.2 Materials and Methods

***Materials.*** Copper chloride ($CuCl_2$; 99.999% trace metals basis (TMB)), europium chloride ($EuCl_3$; 99.99% TMB), scandium chloride ($ScCl_3$; 99.99% TMB), neodymium chloride ($NdCl_3$; ≥99.99% TMB), gallium chloride ($GaCl_3$; ≥99.99% TMB), arsenic chloride ($AsCl_3$; 99.99% TMB), sodium hydroxide (NaOH; 99.99% TMB), hydrochloric acid (HCl; *Trace*SELECT®), and sodium chloride (NaCl; ≥99%) were all purchased from Sigma-Aldrich (St. Louis, MO). Multi-walled carbon nanotube buckypaper filters encapsulated in polyvinyl alcohol were custom-made by NanoTech Labs (Yadkinville, NC). Hydrophilic polytetrafluoroethylene (PTFE; 5μm pore size) membranes and sodium sulfate ($Na_2SO_4$; GR ACS grade) were purchased from EMD Millipore (Darmstadt, Germany).

***Filter Design and Operation.*** In this electrochemical filter device (adapted from Schnoor et al. 2013), voltage was supplied to a CNT filter network to electrochemically precipitate metals (Figure 6.1). Briefly, the filter apparatus was built using a modified 47-mm polycarbonate filter housing (Whatman) with perforated Ti shims acting as the mechanical contact for both the anode and the cathode. Two 47-mm CNT filters were inserted, one as the cathode and one as the anode, with PTFE insulation between. The mechanical contacts were attached to a DC power supply (Agilent E3631A) and test solutions were delivered via a peristaltic pump to maintain a constant flow (Cole-Parmer Masterflex L/S EasyLoad Pump).

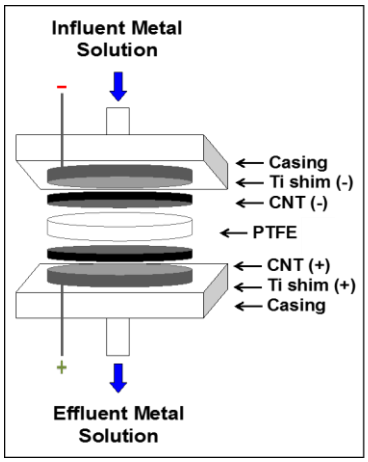


**Figure 6.1.** Schematic of a carbon nanotube (CNT) electrochemical filter device. The system is operated as a multi-stage device in which the applied voltage increases with each filter stacked in series.

***Recovery Optimization: Voltage, Flow Rate, and pH.*** All solutions for the electrochemical experiments were prepared in acid washed glassware (washed for at least one week in 25% v/v HCl followed by one week in 50% v/v $HNO_3$), with 1 mM metal and 100 mM $Na_2SO_4$ (to normalize the ionic strength; Ga was prepared with 100 mM NaCl to avoid precipitation of gallium sulfate ($Ga_2(SO_4)_3$), and tested in triplicate unless otherwise noted. Effluents were collected and quantified for each metal using

inductively coupled plasma mass spectrometry (ICP-MS; Perkin-Elmer ELAN DRC-e). Filters were characterized using scanning electron microscopy (SEM-EDX; Hitachi SU-70 and Hitachi SU-8230 with BRUKER XFlash 5060FQ Annular EDS detector) and analyzed with x-ray photoelectron spectroscopy (XPS; Kratos Axis Ultra DLD) for elemental and metal speciation identification.

The metals/metalloids tested in this study include: Cu, Eu, Sc, Nd, Ga, and As. Note that Cu and Ga were selected as relatively easy to reduce metals, and As as an element known to form stable oxo-anions. All metals were tested over a range of voltages and pH, and three of the five metals (Cu, Eu, Sc) were tested over a range of flow rates to determine the optimum operating parameters to achieve the highest recovery. Note that not all metals were tested across the range of flow rates due to the limited sensitivity to flow rate exhibited by Cu, Eu, and Sc.

Applied voltage ranged from 0.1 V to 3.0 V (depending on the element) while flow rate and pH were kept constant. Keeping flow rate and voltage constant, a wide range of pH values (pH 2-10) were tested, to both ascertain the potential mechanisms of removal and define ranges of function for the device across a range of waste streams with variable pH. Finally, flow rate was tested to determine if typically slow redox kinetics were a limiting step in the recovery process (i.e., if bulk transport past the filter was too fast to allow for metal reduction or precipitation and capture). Here, flow rates ranged from 1 – 5 mL $min^{-1}$ while pH and voltage were held constant. .

***The Role of Oxygen in REE Capture.*** To elucidate the mechanism of ED capture, a single-metal experiment for Eu was conducted without the presence of dissolved molecular oxygen ($O_2$ (aq)). To achieve this, 500 mL of test solution was purged with nitrogen at 200 mL $min^{-1}$ in a 500 mL Erlenmeyer flask with an aeration stone for 90 min before the experiment to ensure no oxygen was present. During the experiment, 5 mL $min^{-1}$ Eu was delivered to the filter at 3.0 V while a constant flow of $N_2$ was pushed into the vacated headspace at 5 mL $min^{-1}$ to maintain neutral pressure and an oxygen-free environment for the duration of the experiment.

***Separations.*** After assessing the behavior of single-metal solutions, a two-stage filter device was assembled to determine whether or not multiple metals could be purified and separated using ED. Cu and Eu were prepared together and the mixed influent solution was pumped into the system containing two filters in series. The upstream filter had an applied voltage of 1.5V to select for Cu and the downstream filter had an applied voltage of 3.0V to select for Eu. The flow rate was held constant at 1 mL $min^{-1}$ and pH was not adjusted (measured pH: 5.4). Effluent was collected and quantified from both filters to calculate recovery.

A real CCR leachate and a synthetic SLM product fluid were delivered to four separate ED filters in series: 0, 1, 2, and 3 V. For the real CCR leachate, EDX-SEM data were collected to assess the qualitative recovery of material at each filter stage. For the synthetic SLM product, ICP-MS was used to calculate recovery and theoretical REE enrichment (wt.%) at each filter stage.

### 6.3 Results and Discussion

***Parameter Optimization.***

***The Effect of Voltage.*** Out of the six metal/metalloids tested here, Cu (selected as an easy-to-reduce metal with a reduction potential of $0.13V_{Ag/AgCl}$) had the highest recovery at 2.0V (87 ± 0.6%), while Ga, Nd, Eu and Sc all exhibited the highest recoveries at 3.0V (in decreasing order: 77 ± 0.4, 72 ± 0.2, 65 ± 0.6, 43 ± 2.8% recovery, respectively (Figure 6.2A; Arsenic data not shown, but it was unrecovered at all voltages). Critically, we note that Ga, Eu, Sc, and Nd did not behave according to their standard reduction potentials to zero-valent metals (Ga: -0.76 $V_{Ag/AgCl}$, Eu: -2.20 $V_{Ag/AgCl}$, Sc: -2.29 $V_{Ag/AgCl}$, Nd: -2.53 $V_{Ag/AgCl}$), where one would anticipate Ga to show the highest recovery, followed by Eu, Sc, and, finally, Nd. Nevertheless, a zero voltage control showed no retained metal on the filters (by SEM, XPS, and confirmed with ICP-MS), indicating *electrochemical activity* was responsible for metal recovery rather than passive collection of natively formed precipitates.

The crystallinity and speciation of the recovered material varied with metal type and, for Cu, as a function of voltage. Crystalline Cu was recovered at 1.5 and 2.0 V, as $Cu_2O$ (i.e., Cu(II) was electrochemically reduced to Cu(I)) (Figure 6.3; XPS data for speciation not shown, but available upon request). In contrast, Ga, Eu, Sc, and Nd formed large plates of amorphous metal, rather than individual metal crystals (Figure 6.3). The REEs were recovered in their trivalent forms as $Ga_2O_3$, $Eu_2O_3$, $Sc_2O_3$, and $Nd_2O_3$. Thus, a mechanism that promoted metal oxide deposition controlled the recovery process, and recovery efficiency would not necessarily improve with increasing standard reduction potential, as observed.

In the absence of pure metal recovery, these data remain encouraging for *selective* recovery of REEs as a mixed cake of metal oxides, where easy-to-reduce or less-soluble oxides are trapped at early filter stages and REEs can be recovered at higher voltage, later stages.

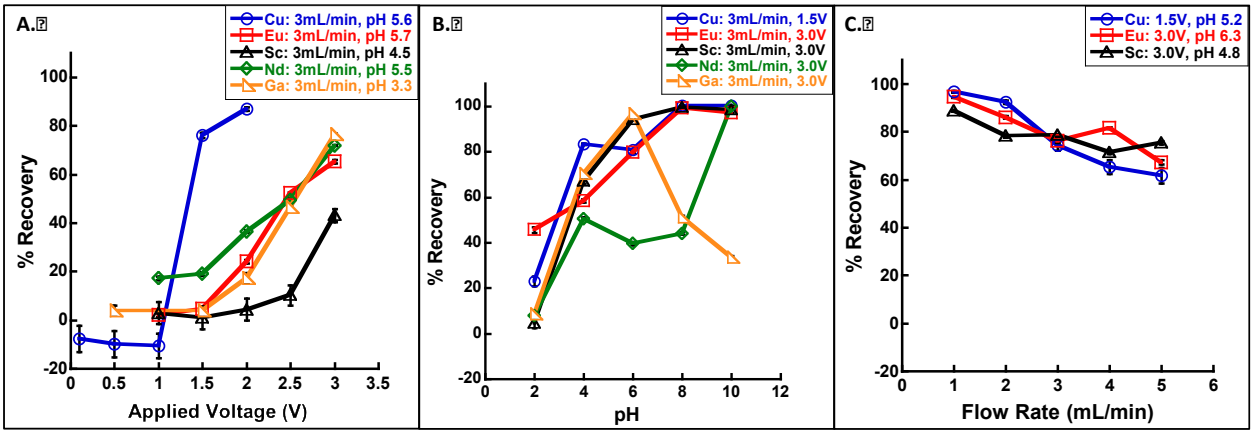


**Figure 6.2.** Recovery of Cu, Sc, Eu and Nd as a function of **(A)** applied voltage (range 0.1-3.0 V), **(B)** pH (range 2-10), and **(C)** flow rate (1-5 mL $min^{-1}$). Blue circles represent Cu, red squares represent Eu, black triangles represent Sc, and green diamonds represent Nd. Note that only one parameter was varied at a time where others were fixed (see legends for details); for (A) the pH was measured after solution preparation rather than titrated to a controlled value. Arsenic (As), which forms stable oxoanions, was unrecovered at all test voltages and pHs.

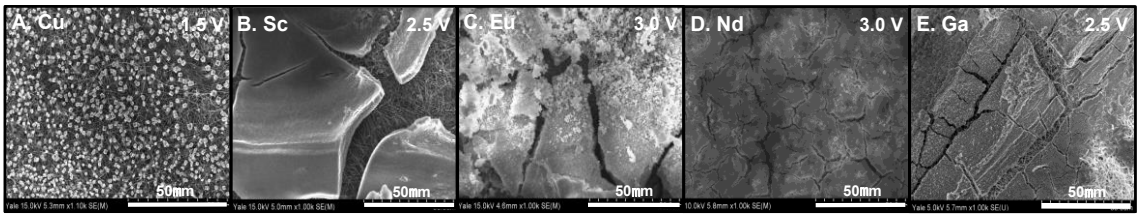


**Figure 6.3.** Representative scanning electron micrographs of **(A)** Cu, **(B)** Sc, **(C)** Eu, **(D)** Nd, and **(E)** Ga at reported voltages. Flow rate was held constant at 3 mL $min^{-1}$ for each metal and pH was 5.6, 4.5, 5.7, 5.5, and 3.3, respectively. SEM data at all voltages and XPS metal speciation for all recovered materials are available upon request.

***The Effect of pH.*** Generally, the recovery of Nd, Eu, Sc, and Cu increased as a function of pH (Figure 6.2B), except for Ga, which exhibited maximum recovery around neutral pH. While one might anticipate these recoveries to reflect changes in solubility (e.g., enhanced formation of metal hydroxides at high pHs), metal hydroxides were not recovered (determined by XPS analysis). Instead, all REEs were recovered as rare earth oxides (REOs; $Eu_2O_3$, $Sc_2O_3$, and $Nd_2O_3$) irrespective of pH (XPS speciation conducted at the extrema of pH 4 and 10). Further investigation was performed to determine the mechanism of recovery (see *Mechanism of Recovery)*, but briefly, we note that CCR leachates (and SLM products) are generally acidic and would have to be adjusted to pH 4 or greater in order to optimize the recovery of REEs.

***The Effect of Flow Rate.*** Cu, Sc, and Eu displayed a sensitivity to flow rate with the highest recoveries at the slowest flow rates (1 mL $min^{-1}$) and lower recoveries at higher flows (4 - 5 mL $min^{-1}$ (Figure 6.2C). This suggested a possible mass transfer limitation, where reduction-mediated trapping was slow compared to bulk fluid transport past the filter at high flow rates. For example, this was reflected in the Cu crystal morphology: near perfect Cu crystals formed at low flow and became less crystalline as flow rate increased (all forms were Cu (I) as $Cu_2O$). Eu and Sc exhibited no visible change in the platelet formation over the flow regime (all forms were trivalent; e.g., $Eu_2O_3$ and $Sc_2O_3$, respectively). This implies more industrially relevant flow rates may come at a sacrifice to *proportionate* metal recovery.

However, the total mass of metal recovered increased with flow rate; i.e., the flux to the surface of the filter was not flow rate limited (Figure 6.4). This is promising for the industrial process, as it suggests that the mass yield could be improved with higher flow velocities and that higher area filter devices could improve recovery flux and potentially yield (see Phase 2 proposal). Note that the effect of concentration on mass flux was also assayed for Cu and Eu, where the mass flux continued to increase with increasing solution concentrations (Figure 6.4B). The proportionate recovery of Eu decreased at the highest concentrations, and this is likely associated with the mechanism of recovery (see below for discussion). Fly ash leachates and SLM product fluids tend to have REE concentrations in the $10^{-8}$ -$10^{-6}$ M range, which exhibited lower proportionate recoveries for Eu.

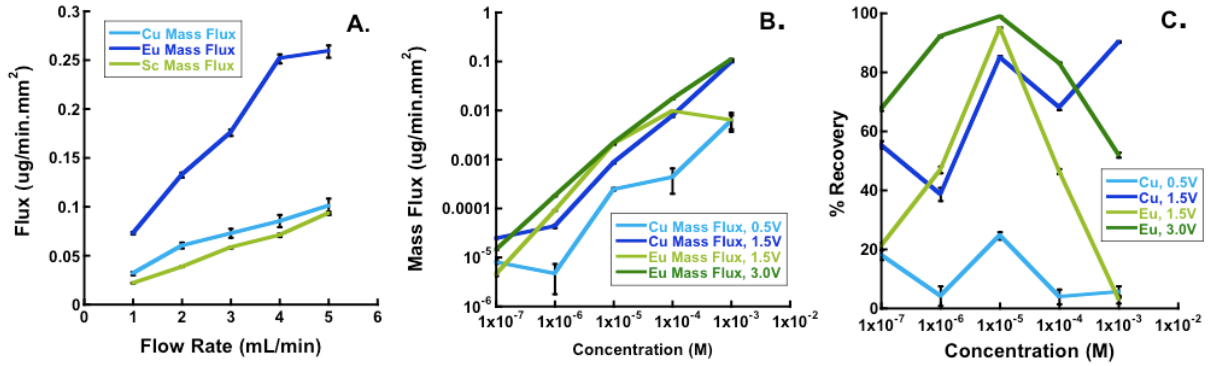


**Figure 6.4.** The mass flux of metal to the filter surface for Eu, Cu, and Sc. Mass flux increased monotonically for Eu, Cu, and Sc over **(A)** 1-5 mL $min^{-1}$ flow rates (data correspond to Figure 6.2C; all $10^{-3}$ M) and **(B)** $10^{-7}$ – $10^{-3}$ M concentrations (for Cu and Eu, corresponding to a range of 6.4 - 63,546 ppb and 15 - 150,950 ppb, respectively). **(C)** Proportionate recovery as a percentage decreased at the highest concentrations for Eu, but not for Cu, and the voltage dependence was greater for Cu. This is consistent with the postulated mechanism of metal recovery (see discussion below), where electrochemical mediated oxide formation for REE capture is limited at the highest metal contents due to lower levels of electrochemical hydroxide formation.

***Mechanism of Recovery.***

Recovery of all REEs was in an oxidized trivalent (e.g., Eu(III)) form, irrespective of pH. REE-oxides could form via two possible electrochemically-dependent routes with distinct oxygen sources: (a) dissolved molecular $O_2$ that is electrochemically activated, or (b) electrochemical water splitting to form $O_2$. To determine the contribution of each, we conducted two unconventional filtration experiments: one purged of dissolved $O_2$ (where oxide formation would be solely due to water splitting), and one purged of $O_2$ with the leads reversed (i.e., where the $O_2$ formed from water splitting, which occurs at the anode, would exhibit enhanced transport to the metal-capture surface at the cathode) (Figure 6.5).

Eu recovery decreased in the absence of $O_2$ from 86 ± 2%, to 34 ± 1%, indicating that dissolved molecular oxygen is an important source of $O_2$, but also that the back diffusion of $O_2$ derived from water splitting at the anode was also substantial (i.e., 40% of the total observed in normal operation) (Figure 6.5A). To confirm the importance of the latter, we qualitatively confirmed the presence of $H_2$ (a necessary co-product of water splitting) through the observation of ignitable $H_2$ (g) evolution and quantitatively determined there was enhanced recovery when the leads were flipped (i.e., the anode on top and the cathode on the bottom to test for enhanced oxygen transport in the direction of the bulk fluid flow; Figure 6.5B). Indeed, recovery of Eu was 56 ± 1% (compared to the 34 ± 1% with normal leads), further supporting the importance of water splitting as a source of $O_2$ for oxide formation and recovery.

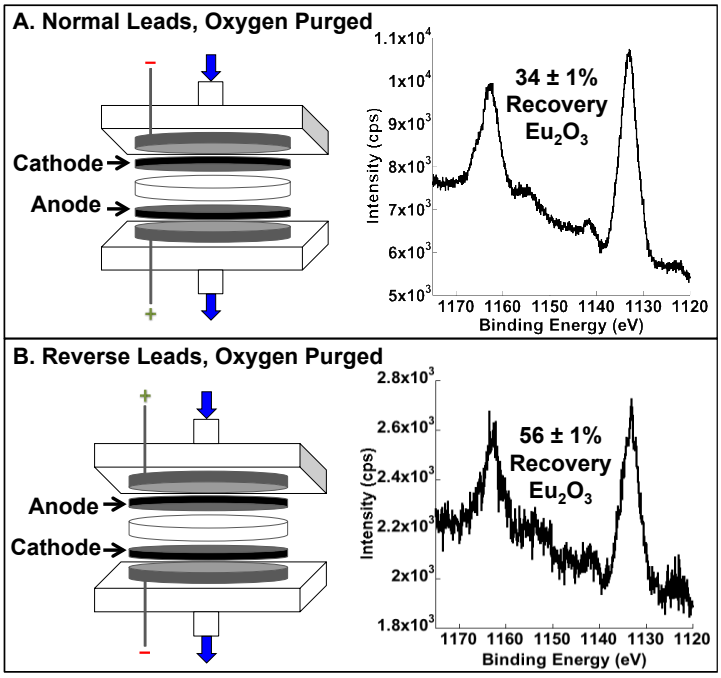


**Figure 6.5.** Schematic of oxygen purge lead arrangement and confirmation of $Eu_2O_3$ formation via x-ray photoelectron spectroscopy. **(A)** Deaerated experiment with normal leads (i.e., cathode on top) with 34±1% recovery, compared to 86 ± 2% in the aerated system, suggesting that nearly 60% of the total recovered in an unaerated sample was due to the presence of dissolved molecular oxygen. **(B)** Deaerated experiment with reverse leads (i.e., anode on top; enhanced $O_2$ transport) with 56±1% recovery. Note: XPS is a surface technique, so the intensity in spectrum (B) is lower (with a correspondingly higher signal-to-noise ratio) due to metal deposition within the filter compared to surface deposition seen in (A).

In order to form the oxide, we propose the oxygen and water are being reduced in solution to hydroxide, forming metal hydroxide species and then dehydrating to the insoluble metal oxide (Therese and Kamath 2000) (Figure 6.6). Our logic follows: previous work has shown that oxygen and water can be reduced in aqueous systems at the cathode (Equations 1 and 2; (Bard et al. 1985, Therese and Kamath 2000, Haynes 2014)), occurring at 0.19 $V_{Ag/AgCl}$ and -1.0 $V_{Ag/AgCl}$, respectively (Chaim et al. 1994a, Chaim et al. 1994b).

Cathodic sources of $OH^-$:

$$O_2 + 2H_2O + 4e^- \Leftrightarrow 4OH^- \qquad (1)$$

$$2H_2O + 2e^- \Leftrightarrow H_2 + 2OH^- \qquad (2)$$

Note that molecular $O_2$ (Eqn 1) can be sourced from both dissolved $O_2$ as well as back-diffusion of $O_2$ formed at the anode (Eqn 3).

Anodic source of $O_2$:

$$2H_2O \Leftrightarrow O_2 + 4H^+ + 4e^- \qquad (3)$$

This $O_2$ is sourced from the oxidation of water (-1.44 $V_{Ag/AgCl}$; Eqn 3). Here, we propose oxygen

formed via water oxidation back-diffuses to the cathode, contributing to further hydroxide formation via oxygen reduction (Eqn 1). This hydroxide could encourage the formation of insoluble metal hydroxides, which could subsequently dehydrate to the observed metal oxides (Figure 6.6).

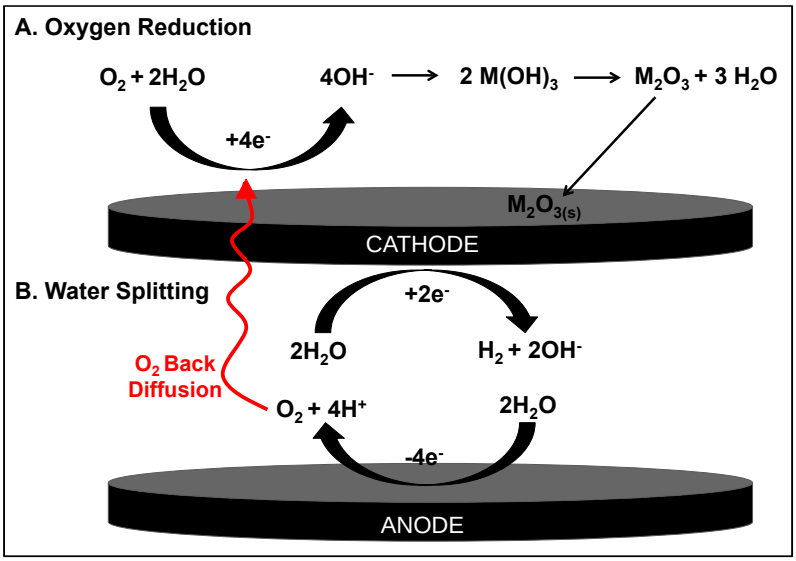


**Figure 6.6** Proposed mechanism for electrochemical deposition of metal oxides (e.g., $M_2O_3$) via a metal hydroxide intermediate (e.g., $M(OH)_3$ for trivalent REEs). Molecular oxygen ($O_2$) can form hydroxide at the cathode through **(A)** oxygen reduction or **(B)** water splitting. Note that water splitting contributes additional molecular oxygen ($O_2$) via anodic water splitting.

The pH dependency supports this hypothesis: in general, metal recovery behaved according to hydroxide solubility (e.g., Ga has high recovery at pH 6 and Eu at pH 10, where the hydroxide forms dominate) (Ames and Rai 1978, Cheng et al. 2012, Paul L. Brown 2016), consistent with the formation of a metal hydroxide intermediate. Arsenic, which forms no insoluble metal hydroxides (and only very soluble oxides), was not recovered at any pH or voltage. Interestingly, the reduction potential of Cu(II) to Cu(0) is similar to the reduction potential for $O_2$ (Eqn 1), 0.13 $V_{Ag/AgCl}$ and 0.19 $V_{Ag/AgCl}$, respectively. In this case, there are competing processes: Cu (II) to Cu(I) reduction, followed by oxide formation, prevailed at low pHs, but the oxygen-mediated mechanism outcompeted this reduction at high pH, where $OH^-$ was abundant (and anodic water splitting should have been enhanced).

Overall, while reduction to zero-valent metal was not observed, some voltage-based discrimination was still possible. In mixed-metal waste streams, we would expect bulk dissolved alkali and alkali earth cations to pass through the filter, whereas metals that form highly insoluble oxides (such as Fe, Al, and Si) should be captured at relatively low voltages. REEs could then be captured as oxides at higher applied potential stages.

***Separation using a multi-ED filter stack.***

We attempted separations from several mixed metal media, including: (1) Relatively pure solutions: (a) of Cu and Eu at 1 mM each and (b) of Eu, Nd, and Sc at 1-0.001 mM, where 1.5

and 3.0 V were used in series as the selective potentials; and (2) The synthetic CCR leachate as shown in Table 5.1: (c) real leachate comprising a heated 6M HCl extraction of Plant DE fly ash (PRB-based) as shown in Figure 3.2, (d) the LEM product of Leachate C, and (e) the SLM product of Leachate A, where 0, 1, 2, and 3V were used in series as selective potentials. Thus far, quantitative results are available for (a), (b), and (e), where qualitative results are available all but the LEM product. Briefly, separation of REE, recovered as REOs, is possible from relatively pure samples (Figure 6.7), and a mixture of Nd, Sc, and Eu demonstrated that mixed REE cakes could be recovered together (Figure 6.8). For test solution (a), 97 ± 0.1 % Cu was recovered on the first stage and 65 ± 0.3 % Eu was recovered on the second stage. For test solution (b), 20, 40, or 90% of each of Nd, Sc, and Eu was recovered on the second stage, at $10^{-5}$, $10^{-4}$, and $10^{-3}$ M, respectively. Note that $10^{-5}$ M is more concentrated than typical leachate, LEM, and SLM product REE concentrations. Qualitatively, we note that some of the added electrolyte cation ($Na^+$ from $Na_2SO_4$) was adsorbed to the metal surface, presumably through coulombic interactions, and that the REE seemed to deposit in series (Eu and Nd, then Sc; Figure 6.8, consistent with expectations from the results shown in Figure 6.2A). This suggest there might be a possibility of independently recovering Sc, the highest value REE, from REEs by using more highly resolved potentials (e.g., 1.5, 2.0, 2.5, and 3.0 V, instead of simply 1.5 and 3.0V as tested here).

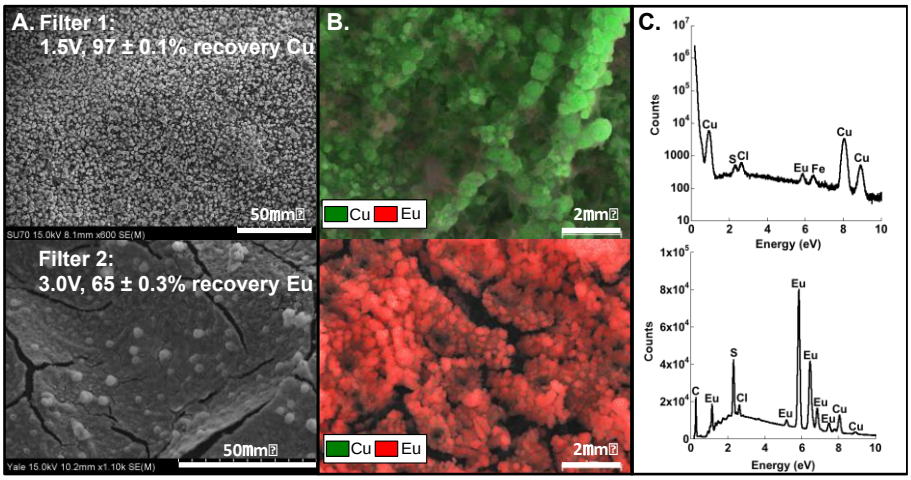


**Figure 6.7.** Characterization of materials collected on a dual filter stage arranged in series from a mixed metal medium containing Cu and Eu: (a) SEM, (b) SEM-EDX mapping, and (c) EDX spectra. The influent solution was prepared with 1 mM Cu, 1 mM Eu, and 100 mM $Na_2SO_4$.

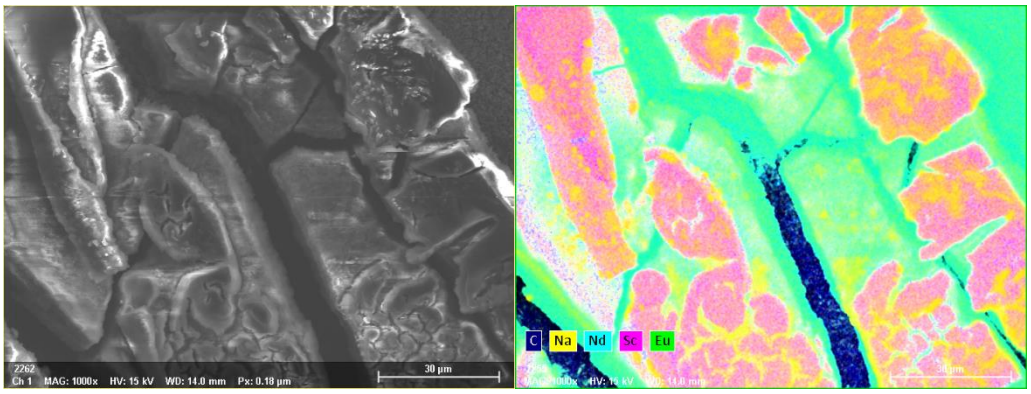


**Figure 6.8.** Characterization of materials collected on a dual filter stage arranged in series from a mixed metal medium containing Eu, Nd, and Sc: (left) SEM, (b) SEM-EDX mapping. The influent solution was prepared with $10^{-3}$ M Eu, $10^{-3}$ M Nd, and $10^{-3}$ M Sc, and 100 mM $Na_2SO_4$. Recoveries were 90% or more for each metal at $10^{-5}$ M, but declined to 40 and 20% at $10^{-4}$ and $10^{-3}$ M, respectively (see Figure 6.4c for concentration dependence data). The scale bar is 30 um, and these platelets are characteristic of the REOs concentrated from pure metal solutions.

For the PRB fly ash HCl leachate charged onto a series of ED filters run at 0, 1, 2, and 3 V, no REEs were observed via SEM-EDX mapping (Figure 6.9), and this is likely due to the high backgrounds of Al, Fe, and Si and trace levels of REEs present in those samples. Indeed, even with high rates of capture of Si, Al, and Fe, breakthrough of these metals/metalloids to subsequent filter stages was significant. Note that REE were quite dilute in the real leachate stream (all less than $10^{-7}$ M, generally less than 150 ppb).

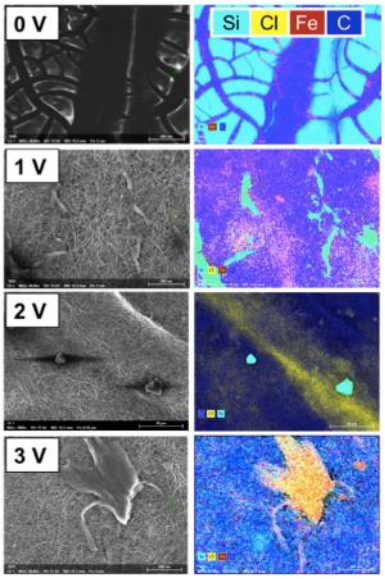


**Figure 6.9.** An HCl leachate of Plant DE fly ash was subjected to a series of ED filters run at increasing applied potentials (0, 1, 2, and 3 V from top to bottom). While large Si platelets were observed on the no and low-voltage filters, Si and Fe breakthrough to high-voltage stages was significant. Note that this real leachate (1) was prepared in HCl, so the $Cl^-$ counterion is visible at all stages and (2) was somewhat aged when used, accounting for the large mass of passively collected material at the 0 V stage.

In order to provide a more concentrated REE starting material for ED, we produced a synthetic SLM product based on the known composition of the SLM product from Leachate A (described in Section 5) and titrated to pH 4. Note that the synthetic SLM product: (1) was used

in place of the real SLM product due to sample volume limitations where the real SLM product was needed to pursue experiments directly related to that objective (see Section 5) and (2) did not contain Si, Th, or U, as accurate quantitation of those elements was not present at the time of the experiment. (Those concentrations are now known and will be included as part of Phase 2 experimentation). Quantitatively, there was an enrichment of the REE on the 2 and 3 V filter stages, whereas the majority of the alkali and alkaline earth cations passed through the filter stack (Figure 6.10). Some Al and Fe were also retained at the 2V stage, where the remainder was either recovered at 0 V (i.e., Al, which likely formed primary or secondary precipitates that were trapped on the 0 V pre filter) or passed through the stack (i.e., the remainder of the Fe). Overall, the ability of the higher-potential filters to trap REEs resulted in a calculated enrichment of solid materials that would be 2.7 wt.% REE (Table 6.1) on the 3V filter. This amount of REE was visible under SEM-EDX, where Tb and Dy were most readily imaged (Figures 6.11 and 6.12). Note this is in contrast to the University of Wyoming team's sample provided courtesy of Prof. M. Fan and Dr. X. Huang, where only Ce, Si, Fe, Al, and C were imaged (data available upon request). Anecdotally, the Wyoming solids are a deep red color, whereas the REOs collected by ED have a white or blue hue). To be clear, Tb and Dy were not necessarily the most abundant REEs in the solid residue, according to the ICP-MS results, but were most readily imaged and clearly assigned by SEM-EDX.

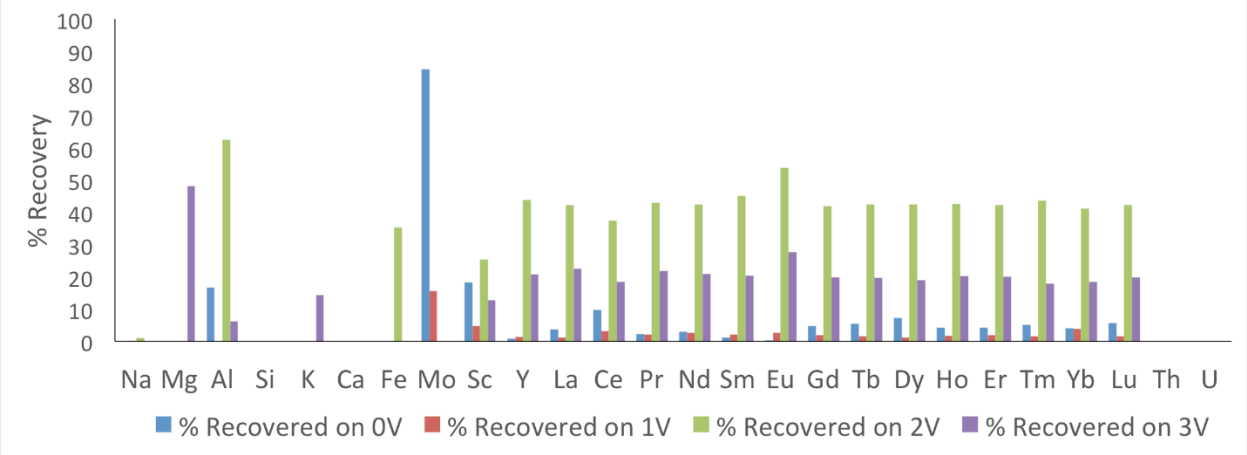


**Figure 6.10.** Proportionate recovery of a suite of bulk and rare earth elements in a synthetic SLM product subjected to a series of ED filters run at 0, 1, 2, and 3 V. Note that Th, U, and Si were not added to the synthetic SLM, but other experiments indicate that the majority of Th may be captured at the 0 V stage, whereas the majority of U passes through the stack (consistent with their expected particle reactivity and solubility; data not shown).

**Table 6.1.** Total mass of material and REE contents in the solids collected on various filter stages after filtration of 150 mL of a simulated SLM product solution from Leachate A. All values were calculated from ICP-MS elemental analysis of the influent and effluent of each filter stage.

| | *0.0 V filter (pre-filter)* | *1.0 V filter* | *2.0 V filter* | *3.0 V filter* |
|---|---|---|---|---|
| Total mass (mg) | 4.4 | 26 | 150 | 0.26 |
| wt.% REE (dry basis) | $3.7 \times 10^{-2}$ | $2.9 \times 10^{-3}$ | $9.5 \times 10^{-3}$ | 2.66 |

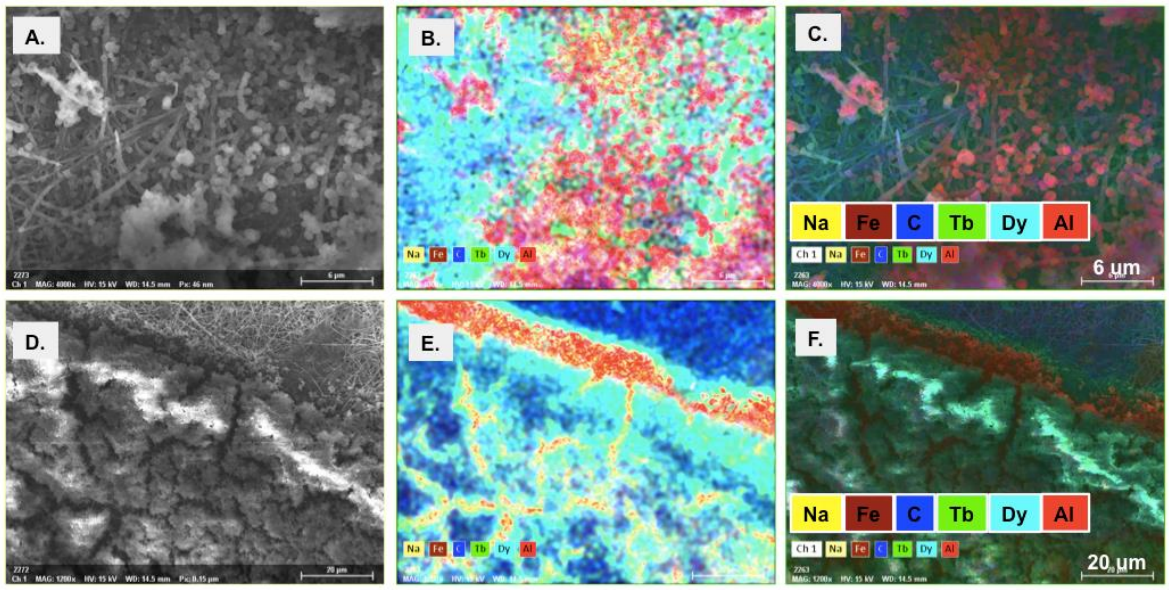


**Figure 6.11.** Material recovered on the 2 V filter was enriched to 0.009 wt% REE and imagable under SEM-EDX, due to the high mass load (150 mg total). **(A-C)** Higher resolution images with a 6 um scale bar; **(D-F)** Lower resolution images with a 20 um scale bar. Panels A and D are traditional SEM, B and E are false color EDX maps, and C and F are depth profile maps. Note that these (A-C versus D-F) are regions of the same 2 V filter, where REE platelets are concentrated on the surface and Al and Fe are focused beneath and/or at the edges of the platelets. $Na^+$, present due to both the CCR extraction process and acid neutralization with NaOH, is visible across the filter surface, but represents only a trace proportion of the influent Na+.

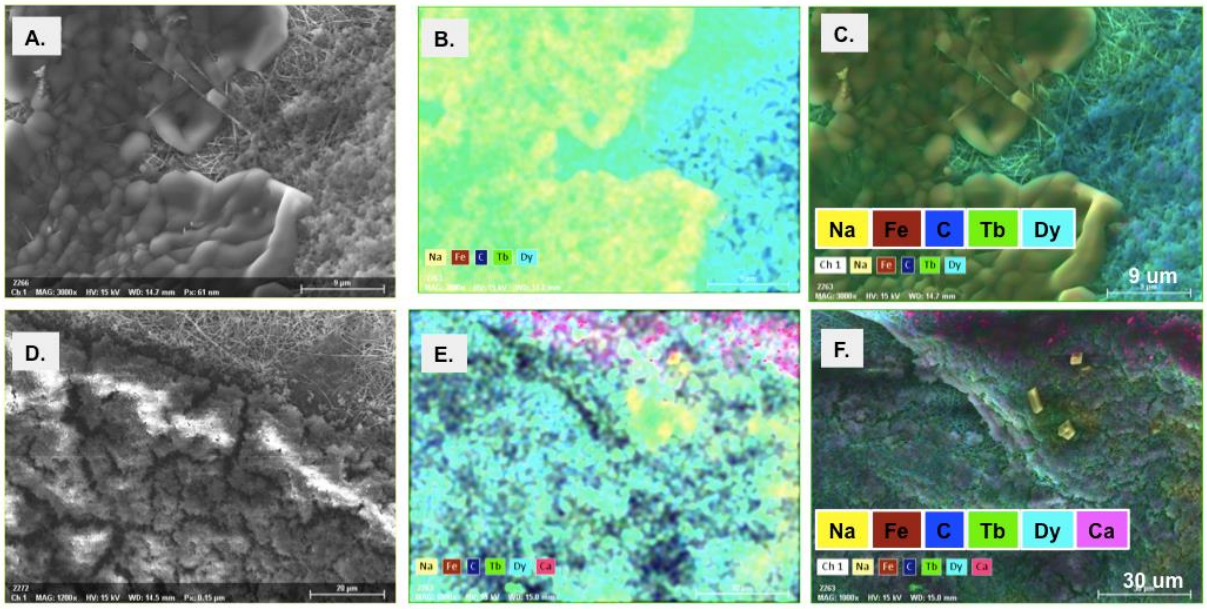


**Figure 6.12.** Material recovered on the 3 V filter was enriched to 2.7 wt% REE and imagable under SEM-EDX. **(A-C)** Higher resolution images with a 9 um scale bar; **(D-F)** Lower resolution images with a 30 um scale bar. Panels A and D are traditional SEM, B and E are false color EDX maps, and C and F are depth profile maps. Note that these (A-C versus D-F) are regions of the same 3 V filter, where REE platelets are concentrated on the surface and Ca and Fe are focused beneath and/or at the edges of the platelets.

Efforts to recover metals from the filters are ongoing, but briefly, we have found that both acetic acid leaching steps (i.e., back flushing or rinsing) and mechanical recovery of the highest mass concentrates are both readily possible. These data are not shown, but are available upon request.

Taken together, the results from the ED experiments are promising to achieve the following technical objectives:

- Separating REEs from bulk alkali and alkali earth cations, which tend to pass through the filter stack (note: no rinse or wash of surface-sorbed ions was attempted)
- There is some discrimination against bulk components Al and Fe, which we expect can be improved with higher resolution of the applied voltages and larger upstream capture areas
- Th and U are expected to be separated from the REEs (data not shown)
- Si is theoretically separatable, but may require larger area upstream (low voltage) filters
- A technique for "drying" the SLM product, which is itself selective for REEs

## 7. Techno-Economic Feasibility Study

The Techno-Economic analysis was based on a preliminary design of an REE recovery operation designed for a basis of 1 ton/hr of ash (dry weight basis). We performed calculations based on the performance of each unit operation as well as a financial analysis that incorporated equipment sizing, capital costs, operational costs, product recovery, and residual disposal costs. Our calculations varied material inputs as well as the unit operations selected for REE recovery. In this effort, the goal was to demonstrate the feasibility of recovering ore at minimum 2% (dry weight basis) mixed REE composition using a range of metallurgic concentration, separation and recovery processes

Our calculations showed that this 2wt% threshold product concentration was feasible. However, the potential for economic viability with REE as the only product was determined to be highly unlikely based on the expected capital and operating costs of several evaluated range of conditions. This is not due to the technology options considered, since based on the low prices for mixed rare earth oxides (~$50,000/yr value of MREO for a feed rate of 1000 kg/hr), it is highly unlikely that any process outside of those under consideration by the team would achieve sustainable economic feasibility. The assessment did show that aluminum is a potential secondary by product as well as highlight areas for cost reduction for each of the process technologies under consideration. Based on the results from the TE analysis, the following recommendations could help guide future work:

i. **Assess technologies and separation methods to individually recover REE elements.** Continuing efforts should be made to evaluate the potential of the electrodeposition process to separate individual REE elements and conduct a technology review to determine the feasibility of co-locating existing REE separation methods. Due to the

likely low value of MREO ore independent of the final concentration, any successful REE recovery approach will very likely need to produce a high quality salable product consisting of pure separated REE or REO. This approach is also common in China, which further supports the need for a complete REE product recovery to ensure economic viability.

ii. **Investigate the approaches to reduce the highest cost driver and/or maximize overall value to the final separation scheme for each of the unit processes:**
    - Alkaline roasting – minimize the roasting agent to ash ratio
    - Acid leaching – minimize acid to coal ash ratio
    - NF – multivalent and monovalent separation factors
    - LEM and SLM – minimize solvent consumption, evaluate alternative for cost
    - Electrodeposition – (1) evaluate the final recovery of REE relative to non-REE constituents for complex mixtures, (2) assess the potential for individual REE separation, and (3) experimentally investigate the minimize required REE concentration in the feed to determine the feed concentration at which a pre-concentration step is required.

iii. **Evaluate the LEM and SLM processes as potential options for final stage REE recovery in addition to assessment as concentration steps.** Both the LEM and UFM processes have potential for high REE recovery and could serve as a terminal collection step for MREE or individual element recovery. Screening and further experimental evaluation of a range of solvent/surfactant consumables with final costs as part of the selection criteria should also be incorporated in continuing efforts.

iv. **Characterize the residual material from each of the lab-scale experiments**. The TE analysis highlighted the potential high costs of waste disposal for the assumed offsite transport and disposal option. This is an area of hte process where operational costs can be greatly reduced by incorporating high levels of reuse and/or onsite treatment to ensure volume reduction.

v. **Perform a review of potential Al recovery technologies that could be incorporated as part of the overall process scheme**. Aluminum was shown to be present in high concentrations in coal ash samples from all regions evaluated. Efficient recovery of Al has the potential to increase the overall feasibility of the MREO process.

Experimental results were used to design a process flow diagram with the following unit operations Alkaline Roasting (optional) → Acid Leaching → Nanofiltration (optional) → Supported Liquid Membrane → Electrodeposition. The key benefits from this configuration are that the final REE solid is projected to contain significantly higher fraction of REE (from 2-9% to 29-79% REE depending on CCR origin) and that scandium is recovered at high purity in the oil phase of the supported liquid membrane system. Figure 7.1 shows the expected annualized product value for this system at the 1000 kg/day scale.

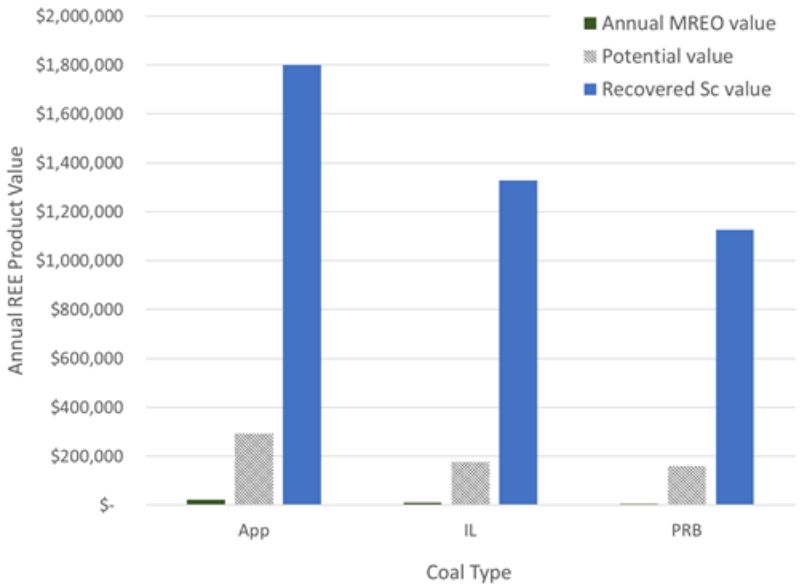


**Figure 7.1.** Projected annualized product value for each coal ash type for the configuration including both NF and SLM process units.

## 8. Conclusions

Key insights that we learned of our process include the following:

- Leaching of REEs from fly ash depends on the feedcoal orgin of the ash, with PRB-based fly ashes requiring  simply a heated acid leaching step for REE extraction while Appalachian and Illinois Basin fly ashes requiring alkaline roasting prior to acid extraction
- Alkaline roasting can be achieved with NaOH (1:1 ratio with fly ash) heated to 450°C for 30 minutes. REEs can leach from this product at room temperature with 0.5 - 1 M $HNO_3$.
- The supported liquid membrane (SLM) system was the best membrane configuration for concentrating REEs from fly ash leachates. The use of mineral oil was equally as efficient as kerosene and could provide advantages with respect to chemical and environmental safety.
- Additional REE concentration steps such as nanofiltration or chemical precipitation can help to further concentrate REEs and separate them from major ions including $Na^+$, $NO_3^-$, $Fe^{3+}$, $Al^{3+}$, and $Si^{4+}$.
- Proof-of-concept testing for the multi-stage CNT-electrodeposition system demonstrated separation and recovery of REEs to a >2 wt.% product from solutions representing the product of SLM separations.
- Economic favorability can be achieved by finding other value streams in the process, such as the recovery of a second Sc-enriched product from the liquid membrane.

## 9. Products

**Publications**

Hood, M. M.; Taggart, R. K.; Smith, R. C.; Hsu-Kim, H.; Henke, K. R.; Graham, U.; Groppo, J. G.; Urine, J. M.; Hower, J. C., Rare Earth Element Distribution in Fly Ash Derived from the Fire Clay Coal, Kentucky. *Coal Combustion and Gasification Products* 2017, 9, 22-33.

Hower, J. C.; Hood, M. M.; Taggart, R. K.; Hsu-Kim, H., Chemistry and petrology of paired feed coal and combustion ash from anthracite-burning stoker boilers. *Fuel* **2017,** *199*, 438-446.

Hower, J. C.; Qian, D.; Briot, N. J.; Henke, K. R.; Hood, M. M.; Taggart, R. K.; Hsu-Kim, H., Rare earth element associations in the Kentucky State University stoker ash. *International Journal of Coal Geology* 2018, 189, 75-82.

Hower, J.C.; Hood, M.M.; Taggart, R.K.; Hsu-Kim, H. (2017). Chemistry and petrology of paired feed coal and combustion ash from anthracite-burning stoker boilers. Fuel. 199,438-446. DOI: 10.1016/j.fuel.2017.03.007

King, J. F.; Taggart, R. K.; Smith, R. C.; Hower, J. C.; Hsu-Kim, H., Aqueous acid and alkaline extraction of rare earth elements from coal combustion ash. *International Journal of Coal Geology* 2018, 195, 75-83.

Mutlu, B. K.; Cantoni, B.; Turolla, A.; Antonelli, M.; Hsu-Kim, H.; Wiesner, M. R., Application of nanofiltration for Rare Earth Elements recovery from coal fly ash leachate: Performance and cost evaluation. *Chemical Engineering Journal* 2018, 349, 309-317.

O'Connor, M.P.; Coulthard, R.M.; Plata, D. L. (2018). Electrochemical deposition for the separation and recovery of metals using carbon-nanotube enabled filters. *Environmental Science: Water Research and Technology* 4, 58-66. DOI: 10.1039/C7EW00187H

Patents:

M.P. O'Connor, C. Vecitis, D.L. Plata. "Electrochemical Separation and Recovery of Metals". Provisional Patent Application No. 62/480,930, filed April 3, 2017. Yale
OCR ref.: OCR 6895

Presentations

Coulthard, R.M.; O'Connor, M.P.; Plata, D.L. "Identification of rare earth elements in electronics waste: Towards advanced-material recycling strategies." 252nd ACS National Meeting & Exposition, Philadelphia, PA. August 21, 2016. Platform presentation.

Couthard, R.; O'Connor, M.; Taggart, R.; Plata, D.; Hsu-Kim, H. Advanced-Material Recycling

Strategies for Rare Earth Elements, Yale University & UMass Boston Green Chemistry Workshop: Metals and Electronics Division. September 1, 2016,

Hood, M.M.; Taggart, R.K.; Smith, R.C.; Hsu-Kim, H.; Groppo, J.G.; Henke, K.R.; Graham, U.M.; Hower, J.C. Rare Earth Element Distribution in Fly Ash Derived from the Fire Clay (Kentucky) Coal. 2017 World of Coal Ash. Lexington, KY. May 8-11, 2017.

Smith, R.C.; Taggart, R.K.;Hower, J.C.; Wiesner, M.; Hsu-Kim. Selective Recovery and Concentration of Rare Earth Elements from Coal Ash Leachate Using Liquid Membranes. 2017 World of Coal Ash. Lexington, KY. May 8-11, 2017.

Hendren, Z.; Choi, Y.C.; Hsu-Kim, H.; Hower, J.C.; Wiesner, M. Preliminary Techno-Economic Evaluation of a Novel Membrane Based Separation and Recovery Process for Rare Earth Elements from Coal Combustion Residues. 2017 World of Coal Ash. Lexington, KY. May 8-11, 2017.

Taggart, R.K.; King, J.F.; Hower, J.C.; Hsu-Kim. Rare Earth Element Recovery from Coal Fly Ash by Alkali Sintering and Leaching Methods. 2017 World of Coal Ash. Lexington, KY. May 8-11, 2017.

Start-up companies:

Nth Cycle LLC. M. O'Connor, CEO (awarded the 2018 DOE Innovation Crossroads)

## 10. References


Ames, L. L., and D. Rai. 1978. Radionuclide interactions with soil and rock media. United States Environmental Protection Agency, Office of Radiation Programs.

Bard, A. J., R. Parsons, and J. Jordan. 1985. Standard potentials in aqueous solution. CRC press.

Bartsch, R. A., and J. D. Way. 1996. Chemical separations with liquid membranes: an overview. ACS Publications.

Chaim, R., S. Almaleh-Rockman, L. Gal-Or, and H. Bestgen. 1994a. Electrochemical Chromium(III) Oxide Coatings on Non-oxide Ceramic Substrates. Journal of the American Ceramic Society **77**:3202-3208.

Chaim, R., G. Stark, L. Gal-Or, and H. Bestgen. 1994b. Electrochemical ZrO2 and Al2O3 coatings on SiC substrates. Journal of Materials Science **29**:6241-6248.

Cheng, T. W., M. L. Lee, M. S. Ko, T. H. Ueng, and S. F. Yang. 2012. The heavy metal adsorption characteristics on metakaolin-based geopolymer. Applied Clay Science **56**:90-96.

Gaikwad, A. G., K. R. Chitra, G. D. Surender, and A. D. Damodaran. 2003. Membrane Solvent Extraction of Some Rare Earth Elements. Chem. Biochem. Eng. Q. **17**:191.

Hasan, M. A., R. F. Aglan, and A. A. El-Reefy. 2009. Modeling of gadolinium recovery from nitrate medium with 8-
hydroxyquinoline by emulsion liquid membrane. Journal of Hazardous Materials **166**:1076-1081.

Haynes, W. M. 2014. CRC handbook of chemistry and physics. CRC press.

Kim, D., L. E. Powell, L. H. Delmau, E. S. Peterson, J. Herchenroeder, and R. R. Bhave. 2015. Selective Extraction of Rare Earth Elements from Permanent Magnet Scraps with Membrane Solvent Extraction. Environmental Science & Technology **49**:9452-9459.

King, J. F., R. K. Taggart, R. C. Smith, J. C. Hower, and H. Hsu-Kim. 2018. Aqueous acid and alkaline extraction of rare earth elements from coal combustion ash. International Journal of Coal Geology **195**:75-83.

Kocherginsky, N., Q. Yang, and L. Seelam. 2007. Recent advances in supported liquid membrane technology. Separation and Purification technology **53**:171-177.

Kulkarni, P., S. Mukhopadhyay, M. Bellary, and S. Ghosh. 2002. Studies on membrane stability and recovery of uranium (VI) from aqueous solutions using a liquid emulsion membrane process. Hydrometallurgy **64**:49-58.

Lauer, N. E., J. C. Hower, H. Hsu-Kim, R. K. Taggart, and A. Vengosh. 2015. Naturally Occurring Radioactive Materials in Coals and Coal Combustion Residuals in the United States. Environmental Science & Technology **49**:11227-11233.

Lichte, F. E., A. L. Meier, and J. G. Crock. 1987. Determination of the rare-earth elements in geological materials by inductively coupled plasma mass spectrometry. Analytical Chemistry **59**:1150-1157.

Meier, A. L., F. E. Lichte, P. H. Briggs, and J. H. Bullock, Jr. 1996. Coal ash by inductively coupled plasma-atomic emission spectrometry and inductively coupled plasma-mass spectrometry. Open File Report 96-525, U.S. Geological Survey, Denver, CO.

Meier, A. L., and T. Slowik. 1994. Rare earth elements by inductively coupled plasma-mass spectrometry. Open File Report 02-223-K, U.S. Geological Survey, Denver, CO.

Paul L. Brown, C. E. 2016. Scandium, Yttrium and the Lanthanide Metals. Pages 225-324 Hydrolysis of Metal Ions. Wiley-VCH Verlag GmbH & Co. KGaA.

Taggart, R. K., J. C. Hower, G. S. Dwyer, and H. Hsu-Kim. 2016. Trends in the rare earth element content of U.S.-based coal combustion fly ashes. **50**:5919-5926.

Therese, G. H. A., and P. V. Kamath. 2000. Electrochemical Synthesis of Metal Oxides and Hydroxides. Chemistry of Materials **12**:1195-1204.

Vandezande, P., L. E. Gevers, and I. F. Vankelecom. 2008. Solvent resistant nanofiltration: separating on a molecular level. Chemical Society Reviews **37**:365-405.